NAE FR 16

NAE FR 16 UNCLASSIFIED

Wing Flow Tests to Determine the Effect of the External Stowage of Four N-44 Missiles on the Lift, Drag and Pitching Moment Characteristics of the Avro CF-100.

16 Apr 53

Spare

L.O. 6664A-3
FILE BM49-7-7
PREPARED BY D.G.G.
CHECKED BY A.D.W.

NATIONAL AERONAUTICAL ESTABLISHMENT
ARNPRIOR, CANADA
LABORATORY MEMORANDUM

SECTION FLIGHT RESEARCH

NO. FR-16
PAGE OF
COPY NO. 10
DATE 16 April, 1953

SECURITY CLASSIFICATION UNCLASSIFIED

SUBJECT

WING FLOW TESTS TO DETERMINE THE EFFECT OF THE EXTERNAL STOWAGE OF FOUR N-44 MISSILES ON THE LIFT, DRAG AND PITCHING MOMENT CHARACTERISTICS OF THE AVRO CF-100

PREPARED BY

D. G. Gould

ISSUED TO

INTERNAL
A. V. ROE (CANADA), MR LINDLEY, 1 COPY
C.A.R.D.E., MR WATSON, 2 COPIES
R.C.A.F, 1 COPY (VIA CARDE)

WING FLOW TESTS TO DETERMINE THE EFFECT OF THE EXTERNAL STOWAGE OF FOUR N-44 MISSILES ON THE LIFT, DRAG AND PITCHING MOMENT CHARACTERISTICS OF THE AVRO CF-100

SUMMARY

Three component balance measurements on the CF-100 half model with two N-44 missiles stowed externally under the nacelle and nacelle-fuselage fillet were made using the wing flow method. A comparison with measurements made with a clean model showed that the effect of the installation on the lift, drag and pitching moment characteristics of the model was within the normal experimental error of the wing flow equipment. It was concluded, therefore, that the effect of the proposed installation on the lift and pitching moment characteristics of the aeroplane would be small.

1. INTRODUCTION

Three component balance measurements were made on the 1/80th scale CF-100 half model with two N-44 missiles located under the nacelle and fuselage-nacelle fillet in order to determine the effect of the installation on the lift, drag and pitching moment characteristics of the model. The location of the missiles on the model is shown in Figures 1 and 2. The missiles were attached to the aircraft model by means of minimum pylons, designed to give sufficient rigidity and minimum interference. The dimensions and location of the pylon relative to the missile are given in Figure 2.

Measurements were made on the model with and without the tail and compared with the results of tests on the clean aircraft given in References 1 and 2.

The nominal tail plane incidence was -2° for the tail-on configuration.

2. SCOPE OF TESTS

Tests were made over the Mach number range from $M = 0.52$ to $M = 0.99$ at two different test altitudes, 10,000 feet and 30,000 feet. The approximate variation of Reynolds number with Mach number for the two altitudes is shown in Figure 3.

The configurations tested were:

a) model without the tail, missiles installed, and
b) complete model, missiles installed.

3. APPARATUS

The N.A.E. transonic wing flow facilities were used to conduct the tests. The model was supported on Driven Balance No. 4 on the port bump. The upper surface of the end plate was 0.1 inches above the bump surface.

4. METHOD

A steady Mach number was established in the flow past the model and the model cycled through twelve degrees angle of attack in one degree steps, the model pausing one-half second at each step.

5. RESULTS

5.1 No-tail Configuration

The results of the tests on the no-tail configuration with missiles installed are given in Figures 4 to 11. The variation of the lift coefficient with angle of attack is given in Figures 4 (a) and 4(b). The lift curve slope, $\frac{dC_L}{d\alpha}$, the value of C_L at which a break occurred in the curve, $C_{L\ Break}$, and the angle of zero lift, α_{L_0}, are plotted against Mach number in Figures 5, 6 and 7. The general effect of the lower Reynolds number (tests conducted at 30,000 feet) on the lift curve slope was to increase $\frac{dC_L}{d\alpha}$ at low Mach numbers and decrease $\frac{dC_L}{d\alpha}$ at the higher Mach numbers. The curve of $\frac{dC_L}{d\alpha}$ against Mach number in Figure 5 shows that the lift curve slope increases from 0.074 at $M = 0.50$ to 0.088 at $M = 0.82$, decreases to 0.052 at $M = 0.84$ and increases again to 0.080 at $M = 0.95$. $C_{L\ Break}$ decreased from 0.56 at $M = 0.52$ to 0.19 at $M = 0.86$ and then increased to 0.40 at $M = 0.95$ (Figure 6). The angle of zero lift shown in Figure 7 stayed approximately constant at -1.75° as the Mach number increased to $M = 0.84$, then suddenly increased to -0.25° at $M = 0.87$, and decreased to -1.1° at $M = 0.93$.

The variation of $C_{M.24\bar{c}}$ with C_L is given in Figure 8. At $M = 0.74$, 0.78, 0.84 and 0.87 there is a considerable change in the aerodynamic centre position as the lift coefficient is increased. At $M = 0.84$ the aerodynamic centre moves aft by 56% of the chord as C_L is increased from .07 to 0.15. At $M = 0.94$ there is a marked hysterisis between the values of $C_{M.24\bar{c}}$ for C_L increasing and C_L decreasing. A similar hysterisis is present in the lift curve at $M = 0.94$ (Figure 4(b)).

$C_{M.24\bar{c}}$ at values of $C_L = 0$ and 0.2 is plotted against Mach number in Figure 9. There is considerable scatter in the results but they indicate that there is a nose-up change of trim of about $\Delta C_M = 0.035$ between $M = 0.85$ and 0.87 at $C_L = 0$. This seems to be associated with the large aerodynamic centre travel shown in the curve of $C_{M.24\bar{c}}$ vs. C_L at $M = 0.87$ (Figure 8).

The drag measurements are given in Figures 10 and 11 where zero lift drag coefficient, C_{D_0}, and the induced drag efficiency factor, "e," are plotted against Mach number. The values of C_{D_0} given in Figure 10 include the drag of the model end plate. The drag of the end plate alone is shown as a dashed curve in Figure 10. Figure 10 indicates that the drag rise starts at $M=0.75$.

The variation of "e" with Mach number given in Figure 11 shows that "e" decreases from 0.72 at M = 0.52 to 0.11 at M = 0.87 and then increases to 0.24 at M = 0.95. The drag data is very sensitive to small zero shifts in the balance chord force direction and is therefore not considered sufficiently reliable to accurately determine the drag rise. Both "e" and C_{D_o} are sensitive to small changes in Reynolds number in the range of Reynolds number within which the tests were conducted.

The results of the present tests on the no-tail configuration are compared with those of Reference 1 for the clean aircraft without a tail in Figures 12 to 17. Comparison of the lift curve slopes with and without the missiles installed is given in Figure 12. The differences between the two curves are not large, no greater in fact than the normal repeatability of the wing flow tests. The curves of $C_{L\ Break}$ against Mach number for the two cases shown in Figure 13 are essentially the same. Figure 14 compares the variation of the angle of zero lift with Mach number for the two cases. The increase in α_{L_o} between M = 0.84 and M = 0.88 is larger by 0.25° with the missiles installed. This difference is no greater than the scatter in the experimental points, however, (see for example Figure 7 of the present memorandum and Figure 5 of Reference 1) so cannot be definitely attributed to the missile installation. The curves of $C_{M.24\bar{c}}$ (at C_L = 0 and 0.2) vs. Mach number for the two cases agree within the accuracy of measurement from M = 0.5 to M = 0.98. Comparisons of C_{D_o} and "e" are given in Figures 16 and 17. The curves of C_{D_o} have been adjusted so that their incompressible C_{D_o}'s have the same value. The drag results are not sufficiently accurate to determine the difference in C_{D_o} or "e" with the missiles installed.

5.2 Complete Aircraft

Plots of the variation of lift coefficient with angle of attack are given in Figures 18 (a) and (b), and the variation of $C_{M.24\bar{c}}$ with C_L in Figures 19 (a) and 19(b). The hysterisis in the C_L vs. α and $C_{M.24\bar{c}}$ vs. C_L curves noted at M = 0.94 for the no-tail configuration is not noticeable in Figures 18 or 19. The $C_{M.24\bar{c}}$ against C_L curves of Figures 19(a) and (b) are linear as C_L increases up to $C_{L\ Break}$ except in the Mach number region from M = 0.82 to M = 0.92, where there is considerable movement of the aerodynamic centre as C_L is increased.

The variation of the lift curve slope and $C_{L\ break}$ with Mach number are compared with the results of References 2 (clean aircraft with a tail) in Figures 20 and 21. In both cases the differences between the curves are not significant compared to the normal scatter of the experimental points through which the faired curves have been drawn.

The angle of zero lift is plotted against Mach number in Figure 22 for the present tests with missiles installed. α_{L_o} increases by 1.3° between M = 0.85 and 0.90 according to this curve and then decreases by 0.6° between M = 0.90 and M = 0.93. Similar data for the clean aircraft was not obtained so no comparison can be made. The changes in α_{L_o} are, however, the same as those observed for the no-tail configuration (Figure 14).

$C_{M_{o}}$ $_{.24\bar{c}}$ at $C_L = 0.2$ and $C_L = 0.2$ is plotted against Mach number in Figure 23 for the model with and without missiles. The curves are similar for the two cases except for a general shift amounting to an increment in $C_{M_{o}.24\bar{c}}$ of about .034 at low Mach numbers. A difference of tailplane setting between the two tests of approximately 0.6^{o} could account for the change in $C_{M_{o}.24\bar{c}}$. It is expected, however, that the tailplane setting between flights would not be different by more than 0.25^{o}, so that the results of Figure 23 indicate that the installation of the missiles causes a small nose down change in $C_{M_{o}}$.

6. CONCLUSIONS

Three component balance measurements on the CF-100 half model showed that in general the effects of the proposed N-44 installation on the lift, drag and pitching moment characteristics of the model were within the normal experimental error of the wing flow equipment. It was concluded, therefore, that the effects of the proposed missile installation on the lift and pitching moment characteristics of the aeroplane would be small.

REFERENCES

1. Gould, D.G. Lift and Pitching Moment Measurements of the Avro CF-100 Half Model, M = 0.3 to M = 1.0. N.A.E. Lab. Memorandum FR-10, Nov. 17, 1952.

2. Gould, D.G. Wing Flow Tests to Determine the Lift, Drag and Pitching Moment Characteristics of the Avro CF-100 Half Model Without a Tail: M = 0.51 to M = 0.98. N.A.E. Lab. Memorandum FR-10(c), April 15, 1953.

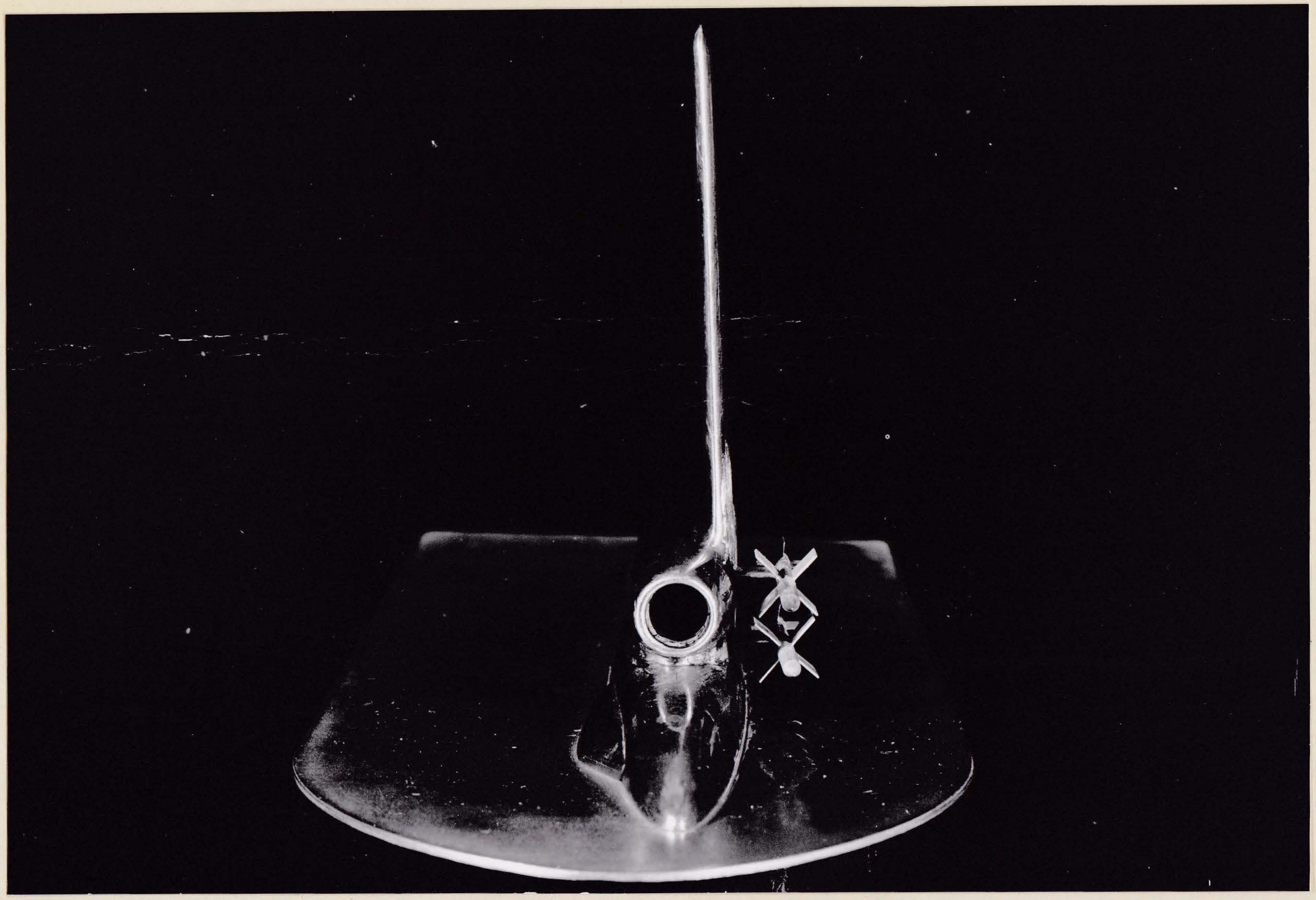

CF—100 HALF MODEL WITH TWO N-44 MISSILES INSTALLED — MINIMUM PYLONS

FIG. 1

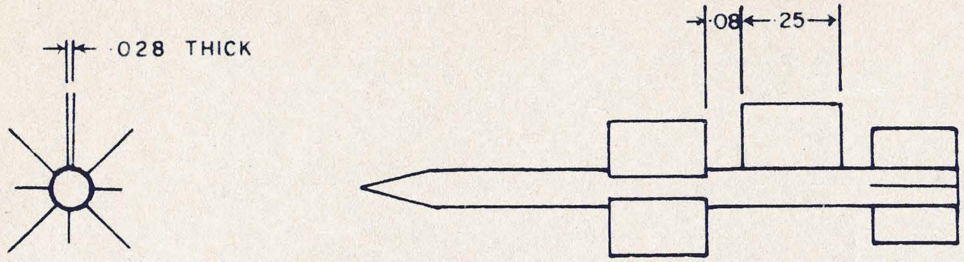

LOCATION AND SIZE OF MINIMUM PYLON

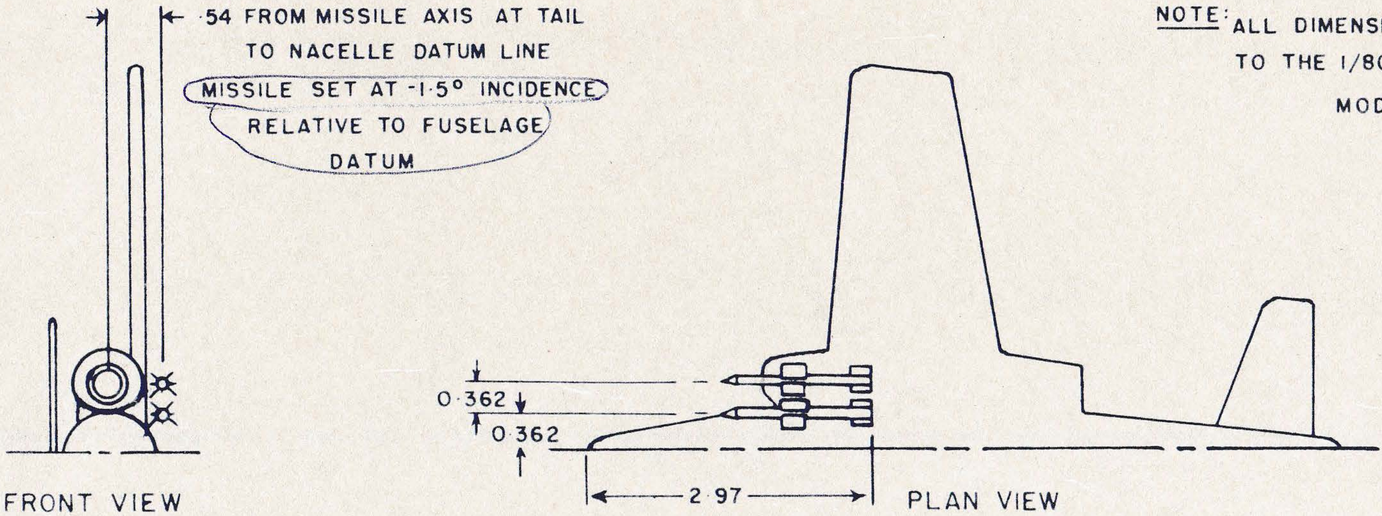

FRONT VIEW

PLAN VIEW

NOTE: ALL DIMENSIONS REFER TO THE 1/80 TH SCALE MODEL

LOCATION OF MISSILES ON HALF MODEL

FIG. 2

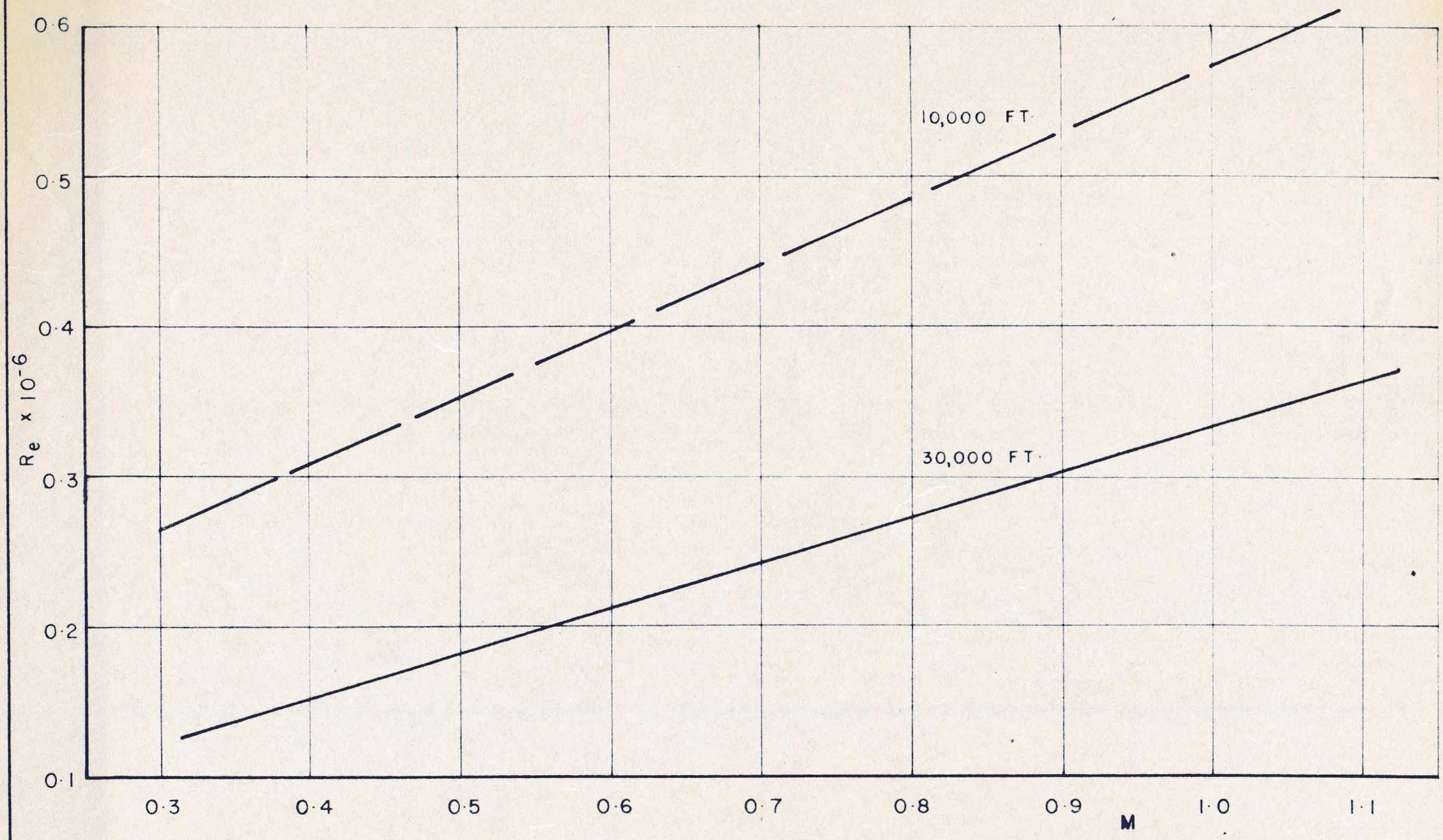

APPROXIMATE VARIATION OF REYNOLDS NUMBER WITH MACH NUMBER

FIG. 3

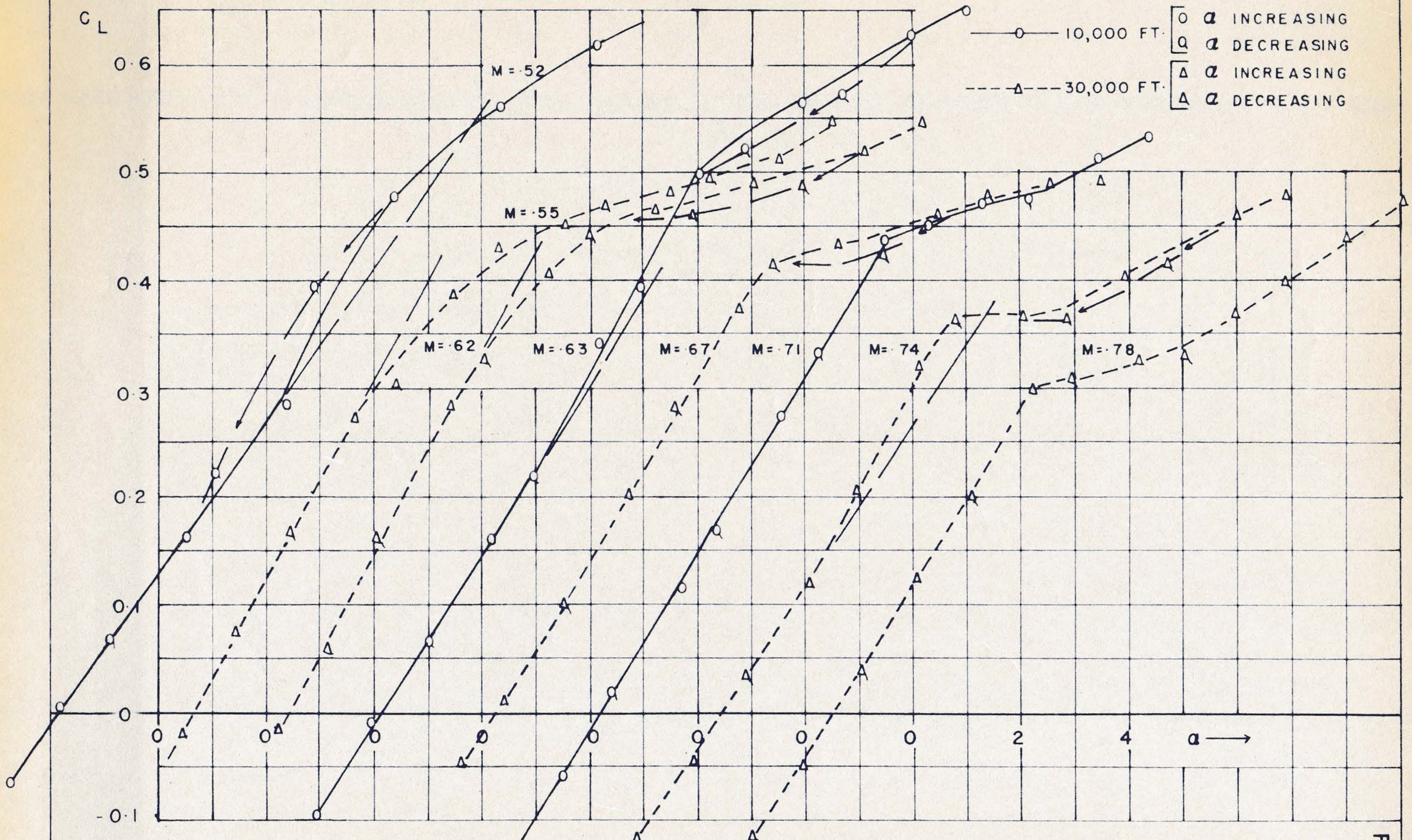

VARIATION OF LIFT COEFFICIENT WITH ANGLE OF ATTACK
NO TAIL CONFIGURATION — MISSILES INSTALLED

FIG. 4 (a)

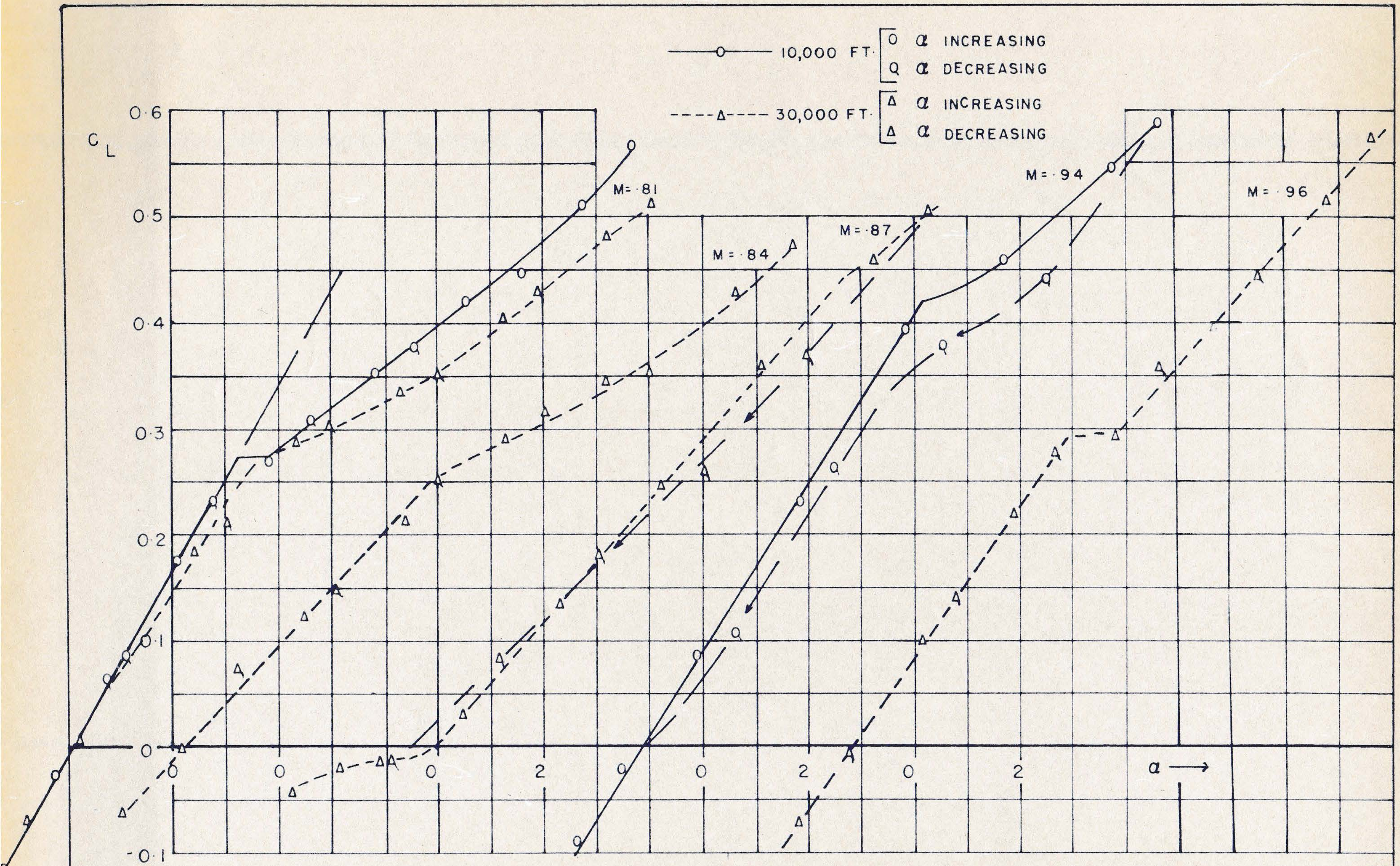

VARIATION OF LIFT COEFFICIENT WITH ANGLE OF ATTACK
NO TAIL CONFIGURATION — MISSILES INSTALLED

FIG. 4(b)

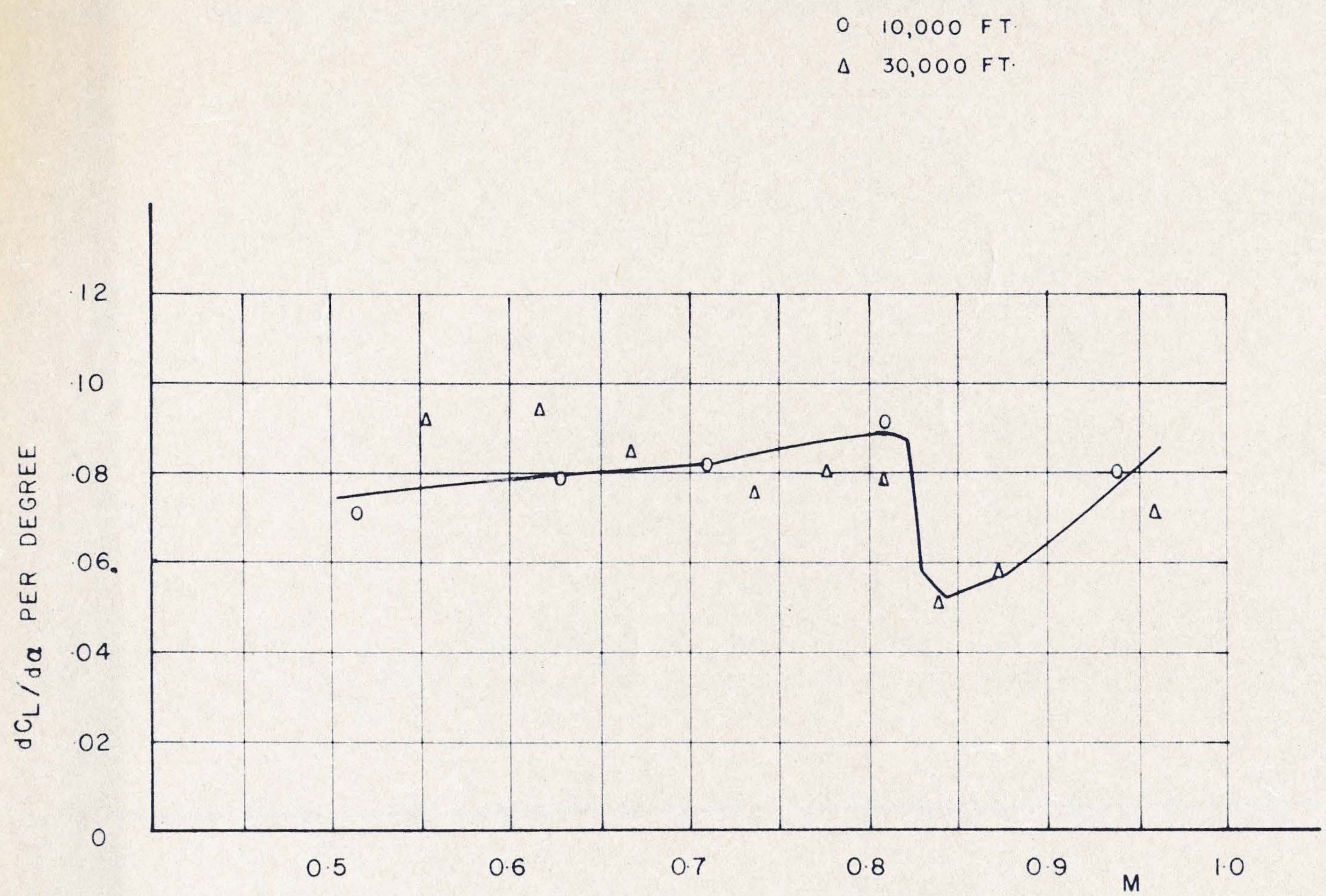

VARIATION OF LIFT CURVE SLOPE WITH MACH NUMBER

NO TAIL CONFIGURATION — MISSILES INSTALLED

FIG. 5

FIG · 6

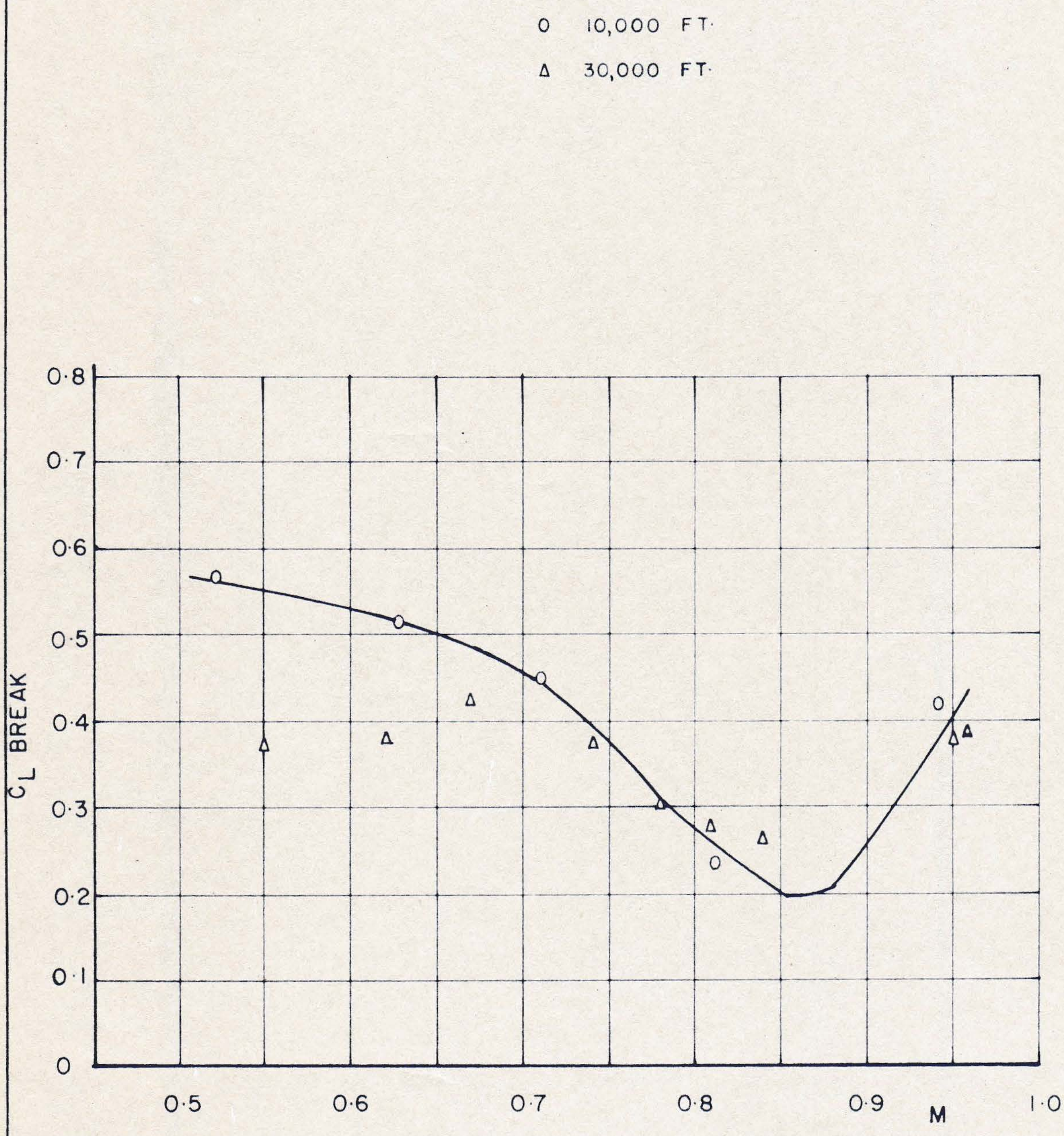

VARIATION OF LIFT CURVE BREAK WITH MACH NUMBER

NO TAIL CONFIGURATION — MISSILES INSTALLED

FIG· 7

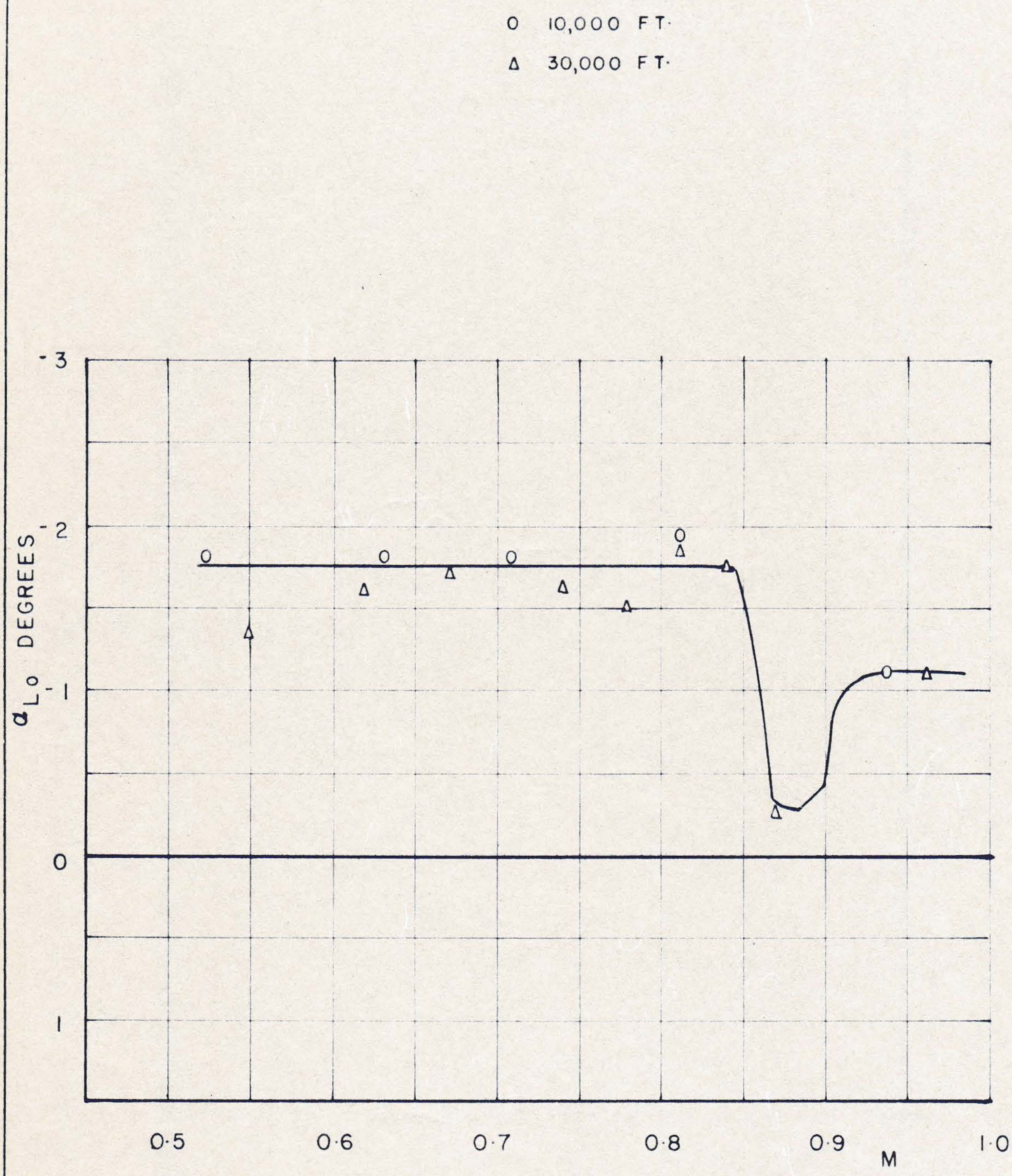

VARIATION OF ANGLE OF ZERO LIFT WITH MACH NUMBER

NO TAIL CONFIGURATION – MISSILES INSTALLED

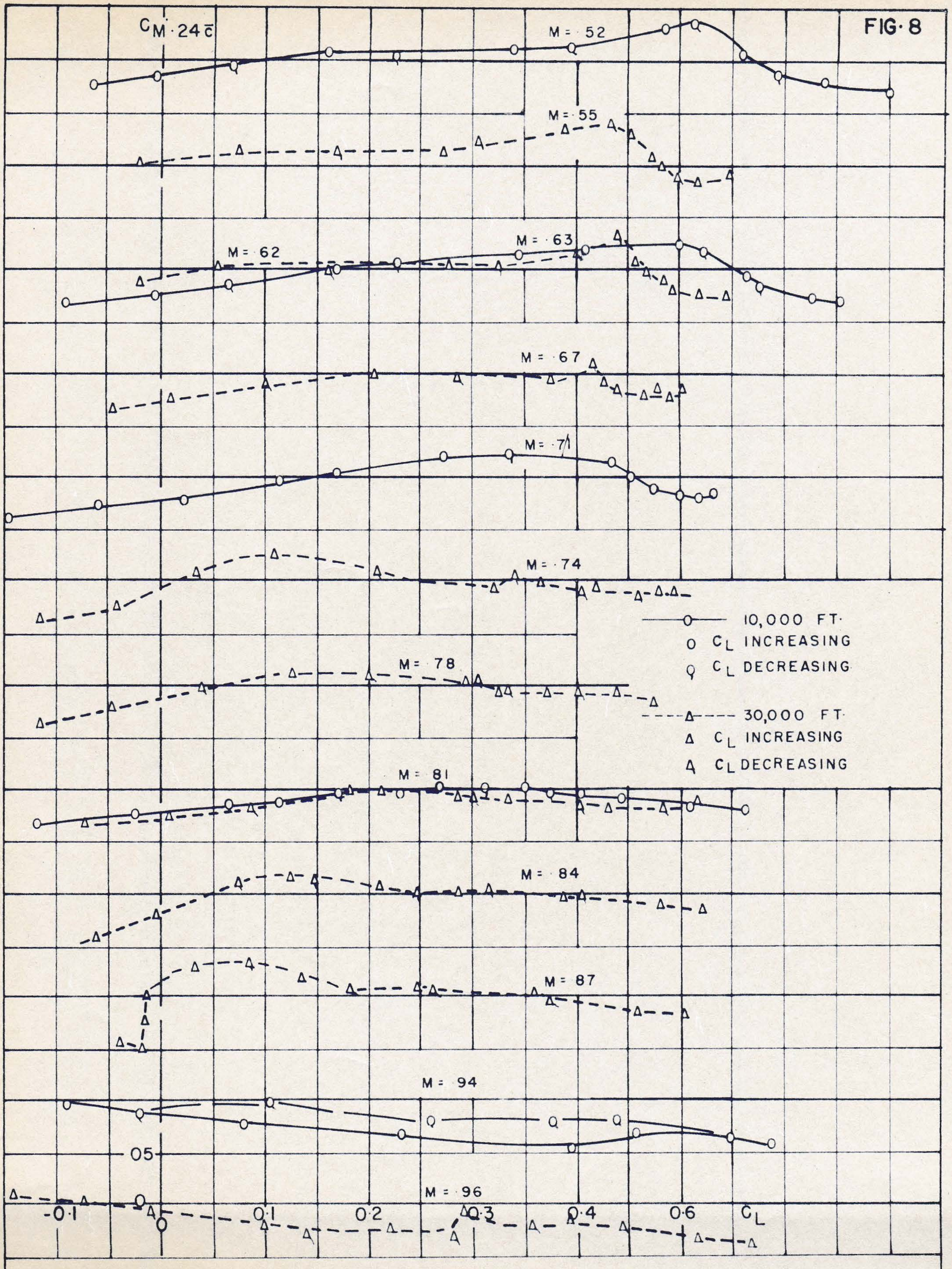

FIG·8

VARIATION OF $C_{M \cdot 24 \bar{c}}$ WITH C_L – NO TAIL CONFIGURATION – MISSILES INSTALLED

FIG. 9

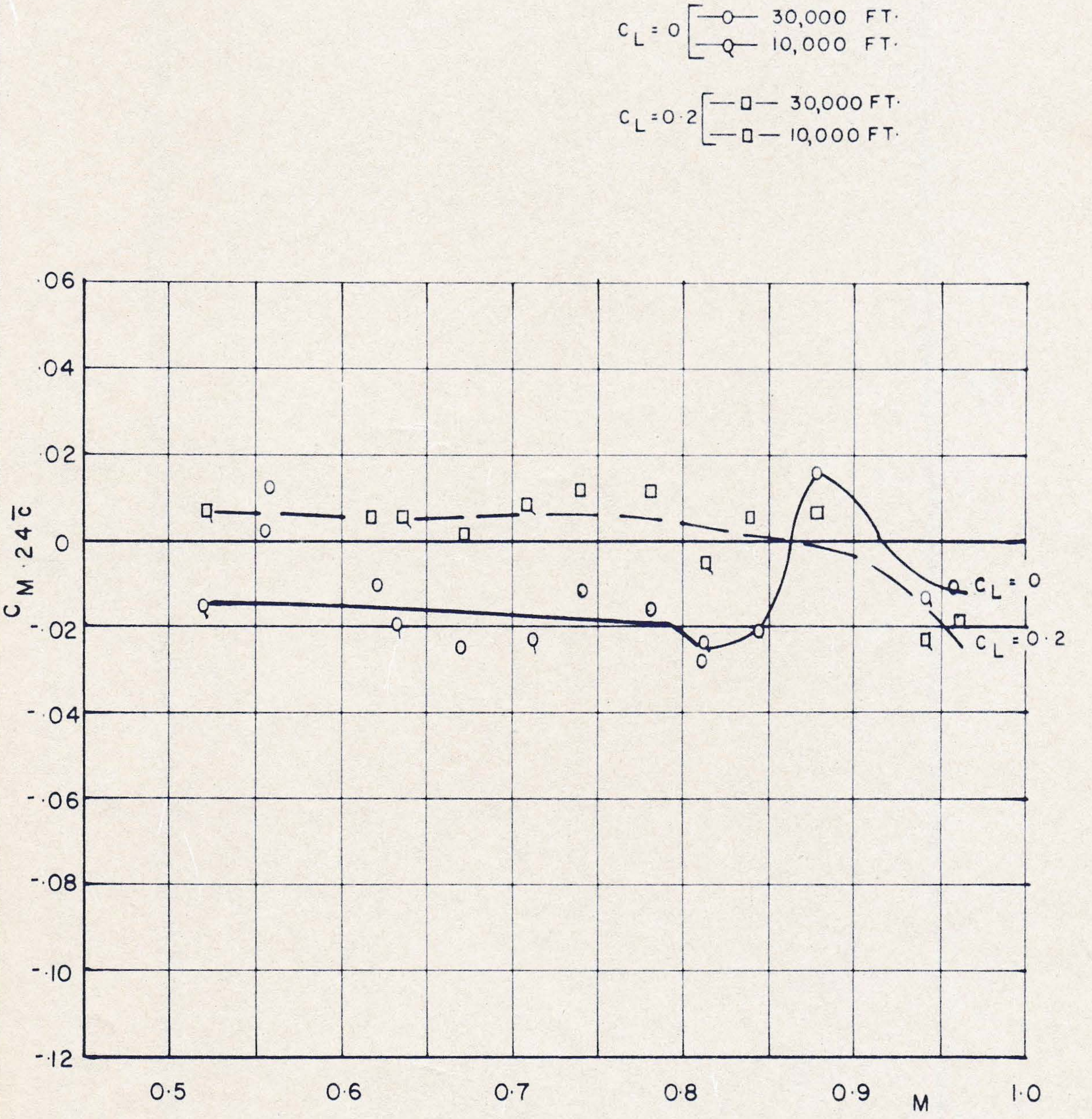

VARIATION OF $C_{M \cdot 24\bar{c}}$ (CONSTANT C_L) WITH MACH NUMBER

NO TAIL CONFIGURATION — MISSILES INSTALLED

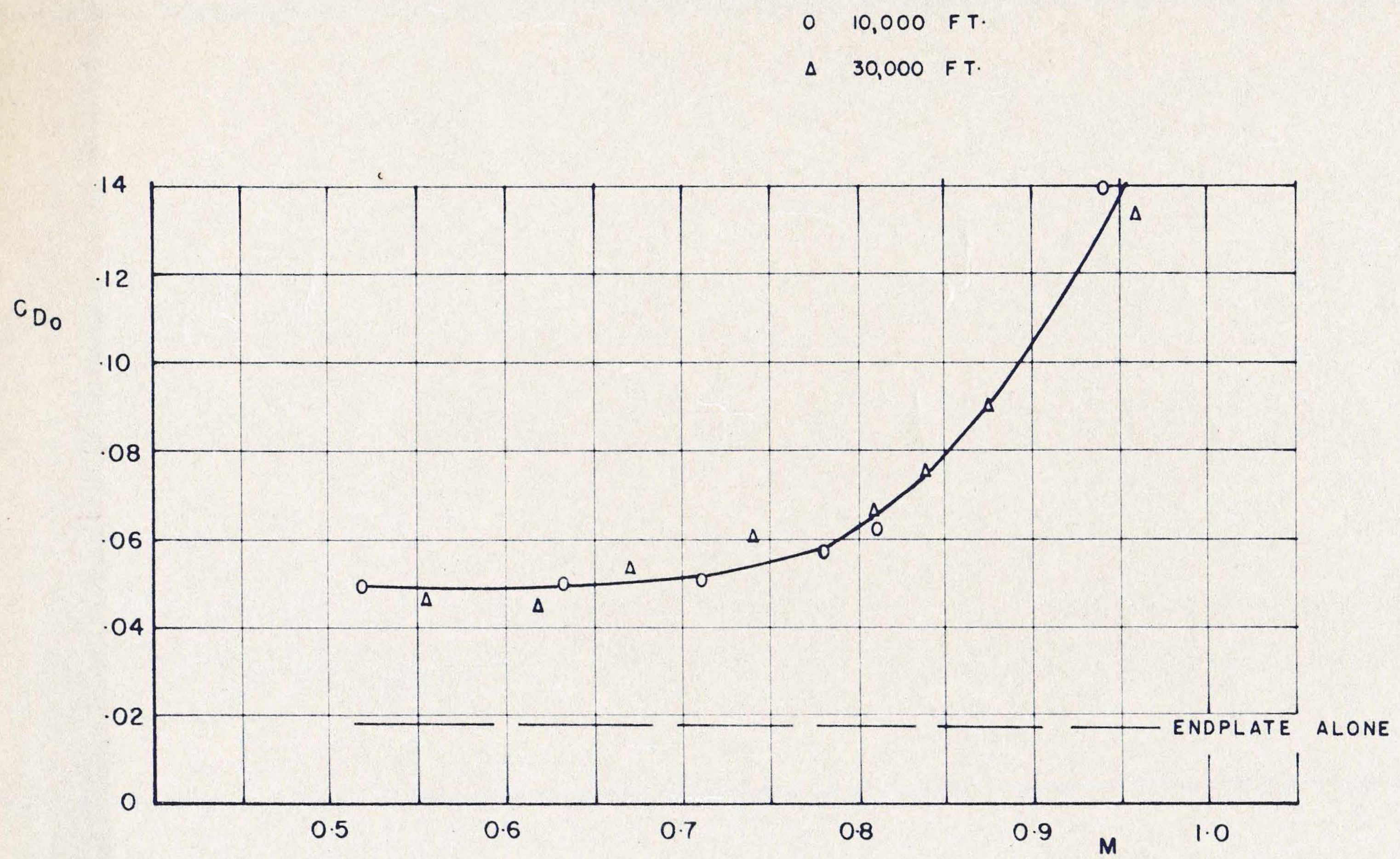

VARIATION OF ZERO LIFT DRAG COEFFICIENT WITH MACH NUMBER

NO TAIL CONFIGURATION – MISSILES INSTALLED

FIG·10

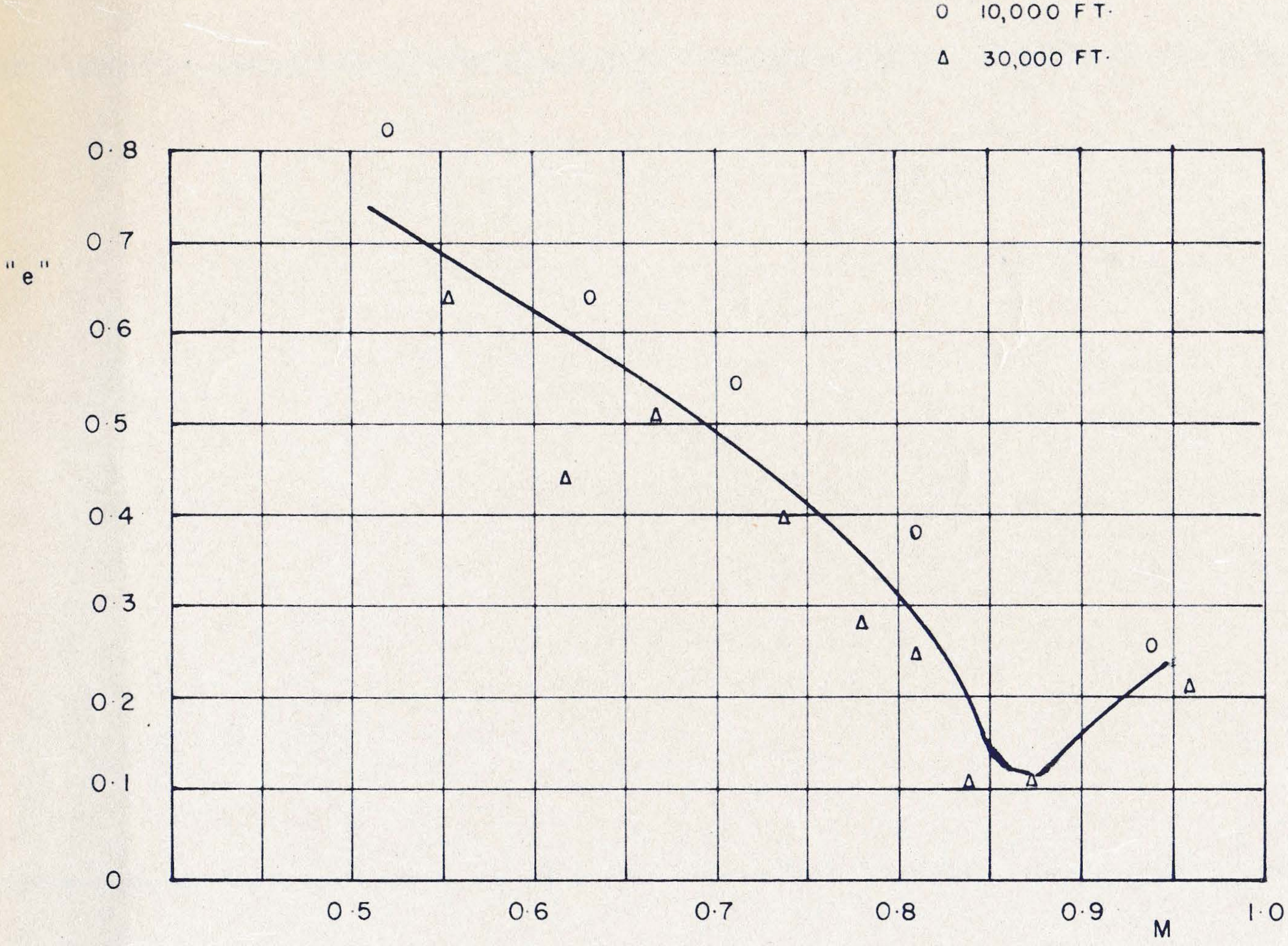

VARIATION OF INDUCED DRAG EFFICIENCY FACTOR "e" WITH MACH NUMBER

NO TAIL CONFIGURATION — MISSILES INSTALLED

FIG· 11

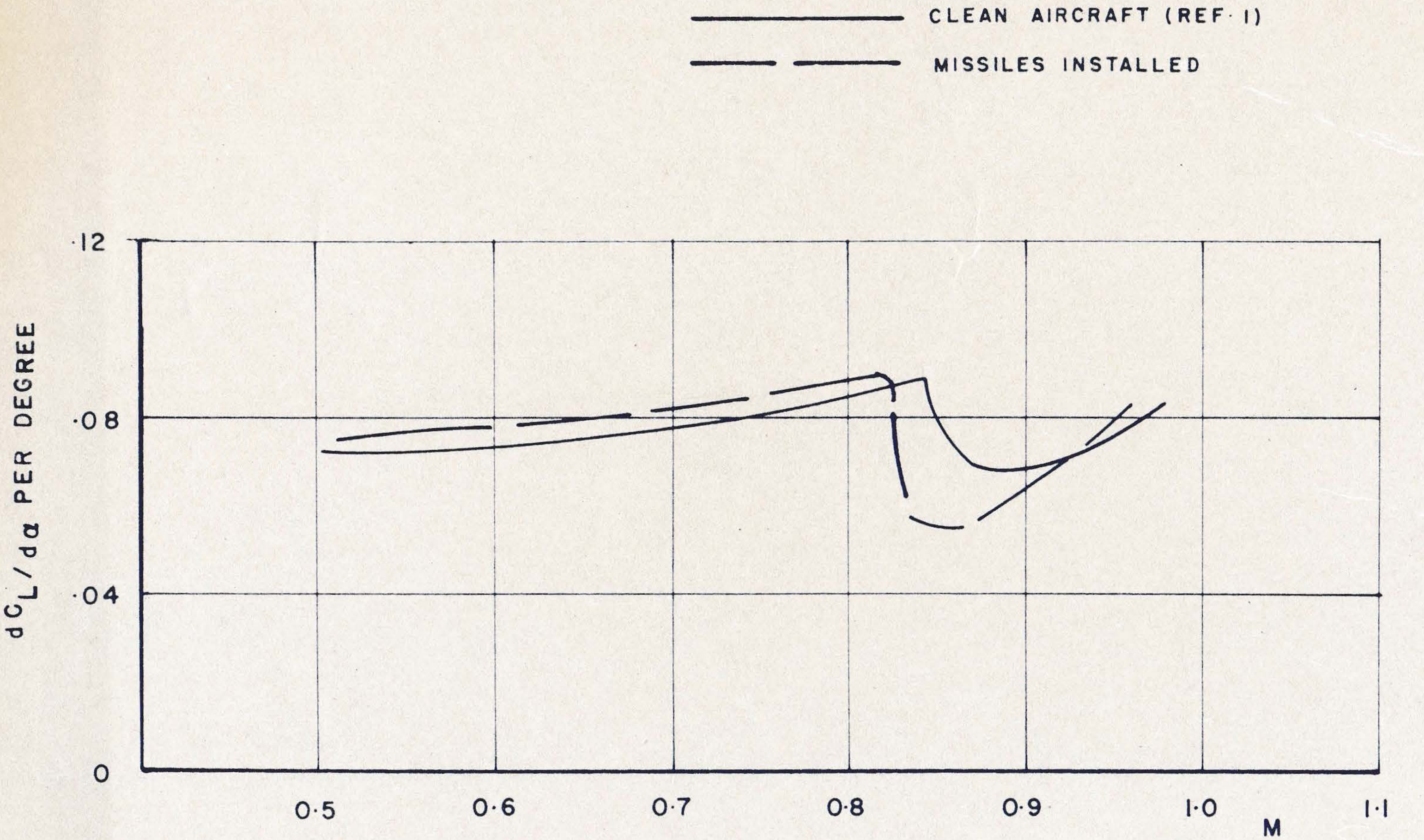

COMPARISON OF LIFT CURVE SLOPES WITH AND WITHOUT MISSILES

NO TAIL CONFIGURATION

FIG·12

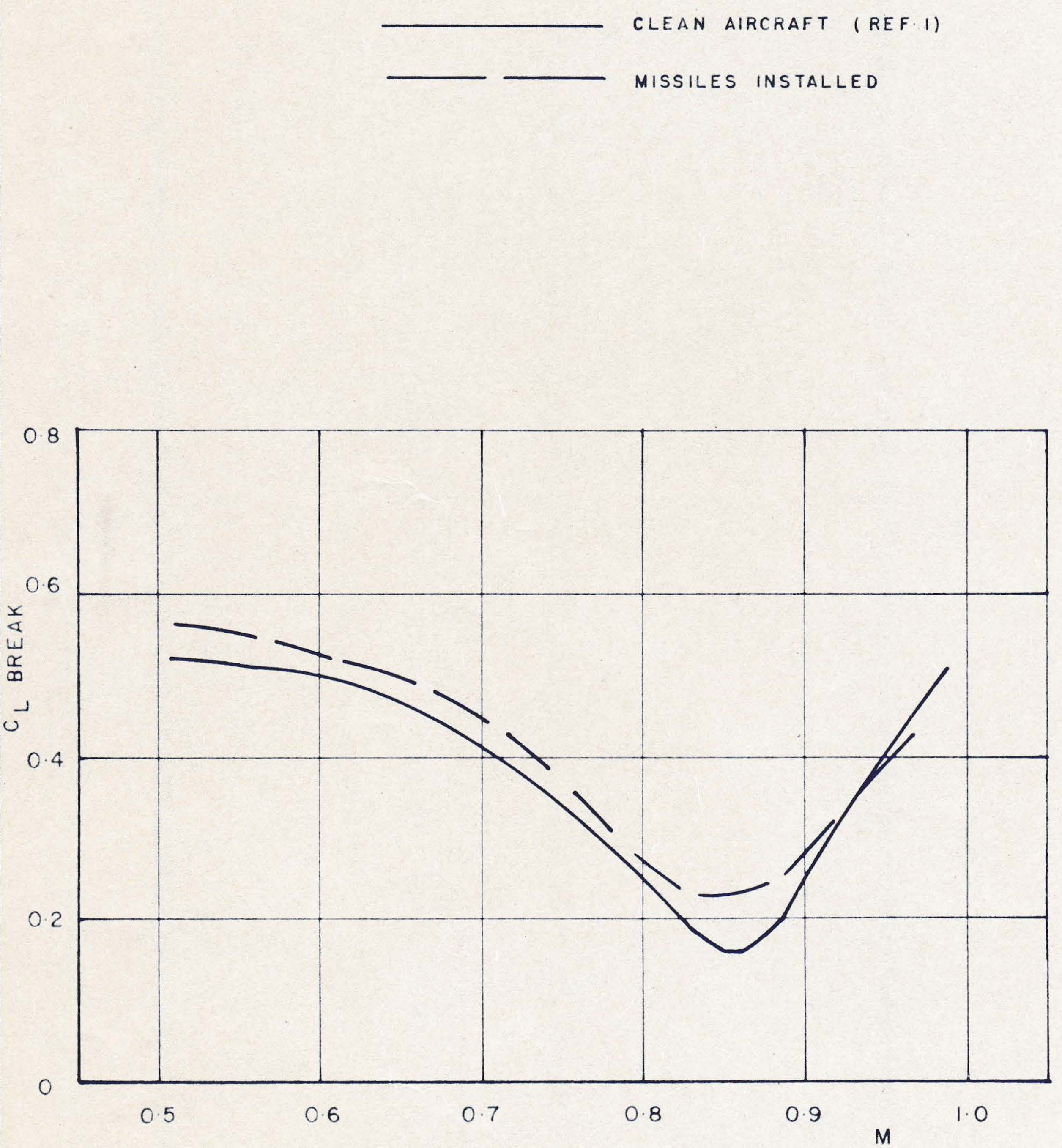

COMPARISON OF LIFT CURVE BREAK WITH AND WITHOUT MISSILES

NO TAIL CONFIGURATION

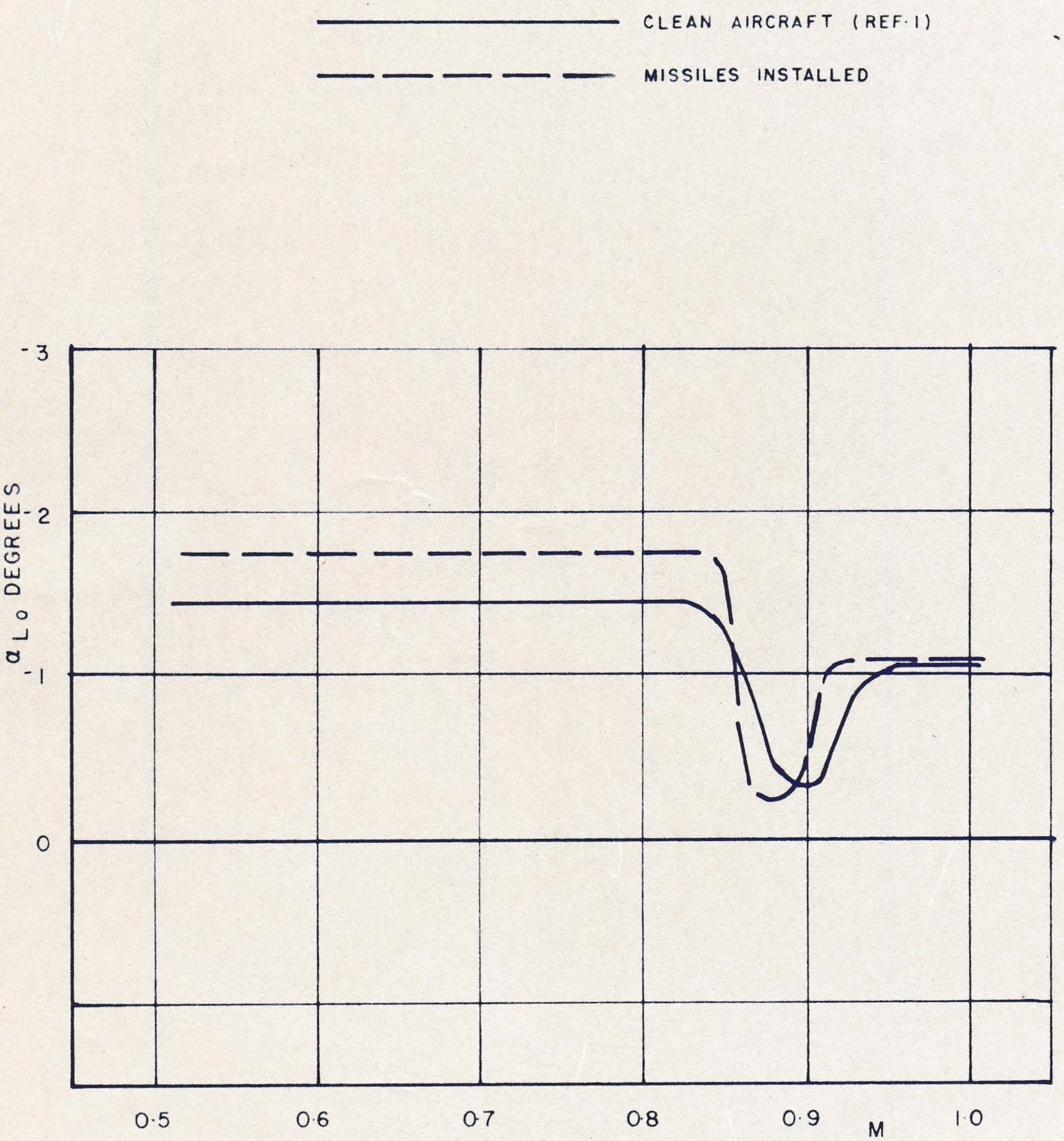

COMPARISON OF ANGLES OF ZERO LIFT WITH AND WITHOUT MISSILES

NO TAIL CONFIGURATION

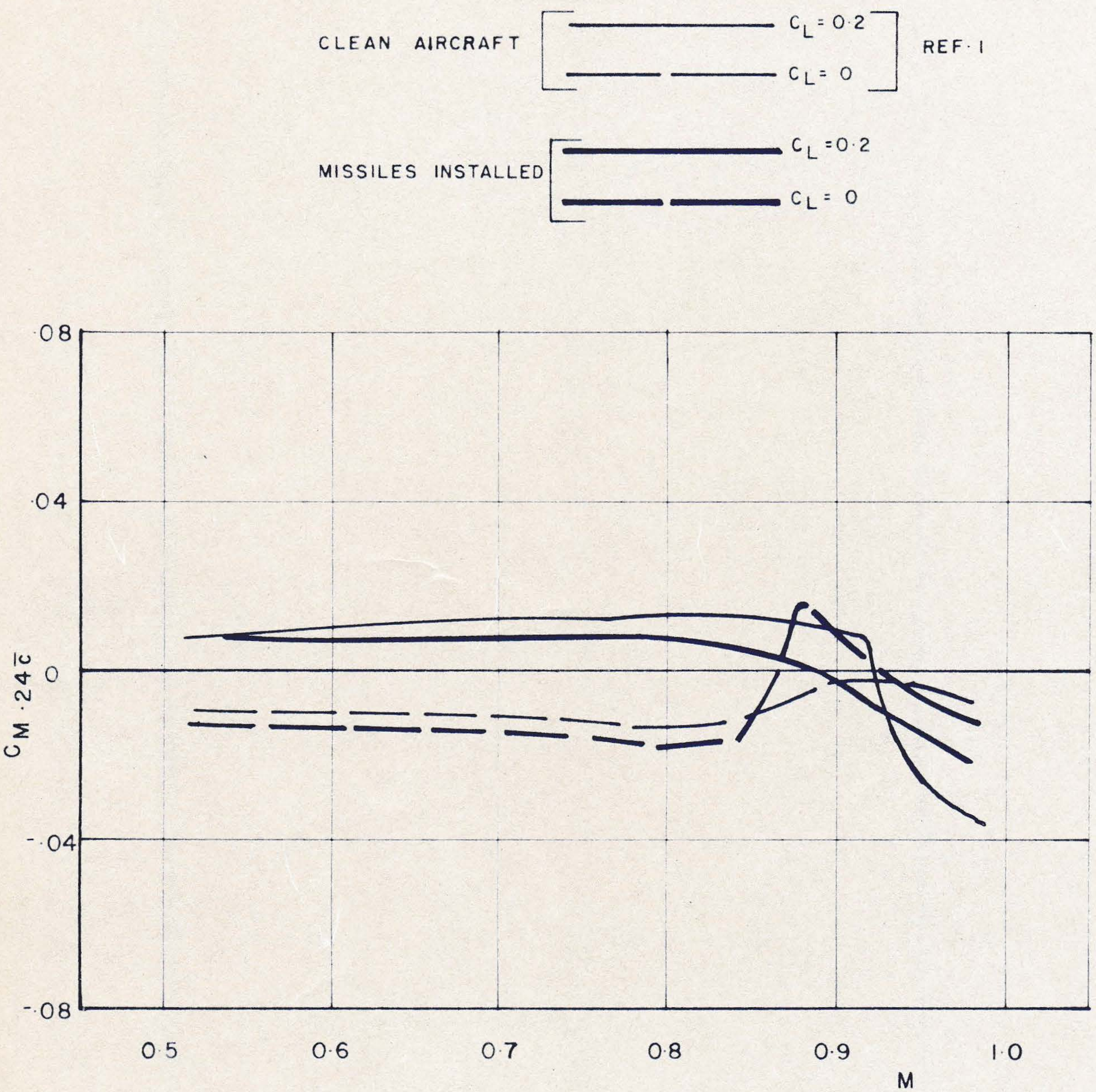

COMPARISON OF $C_{M.24\bar{c}}$ (CONSTANT C_L) WITH AND WITHOUT MISSILES

NO TAIL CONFIGURATION

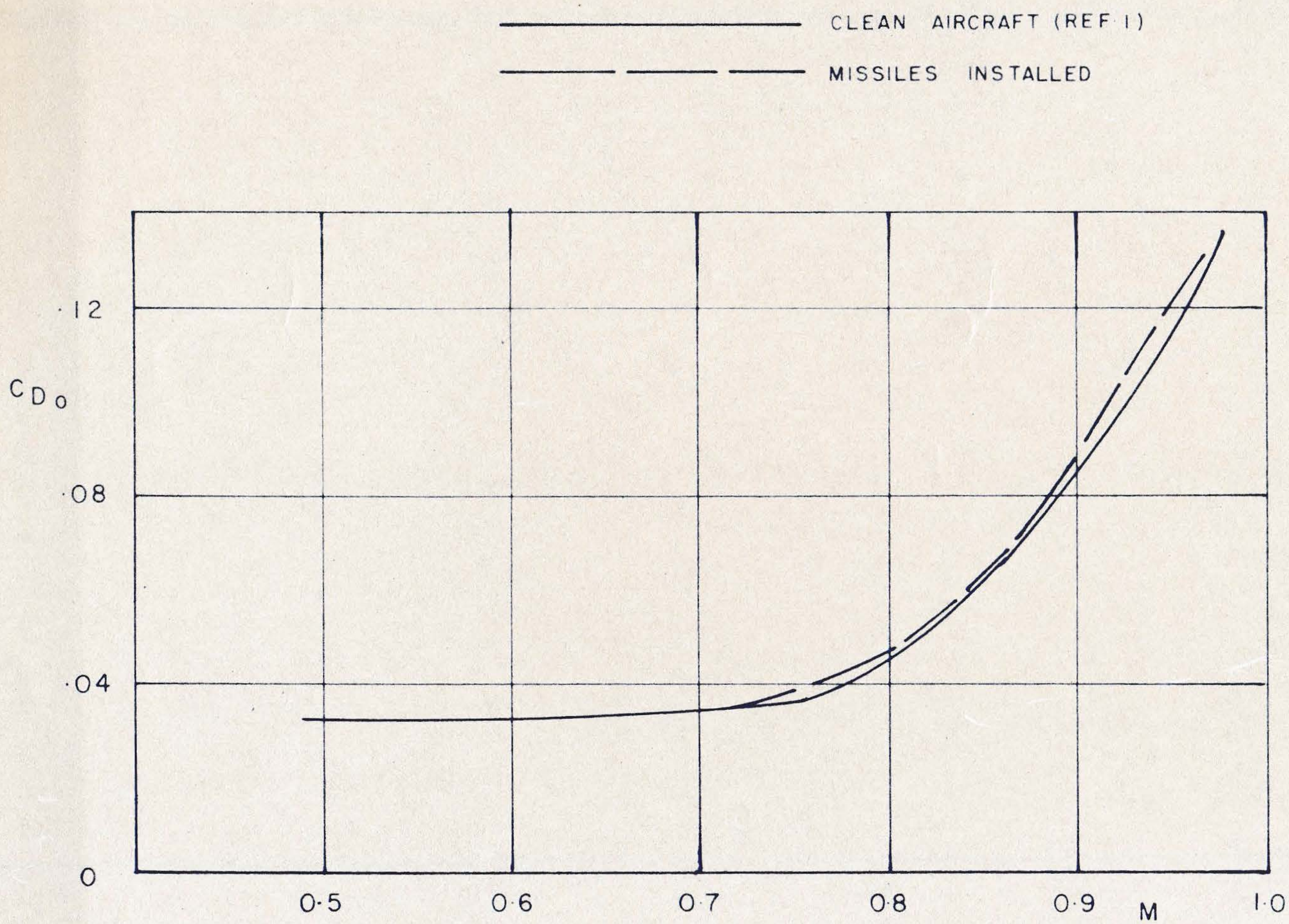

COMPARISON OF ZERO LIFT DRAG COEFFICIENTS WITH AND WITHOUT MISSILES

NO TAIL CONFIGURATION

FIG·16

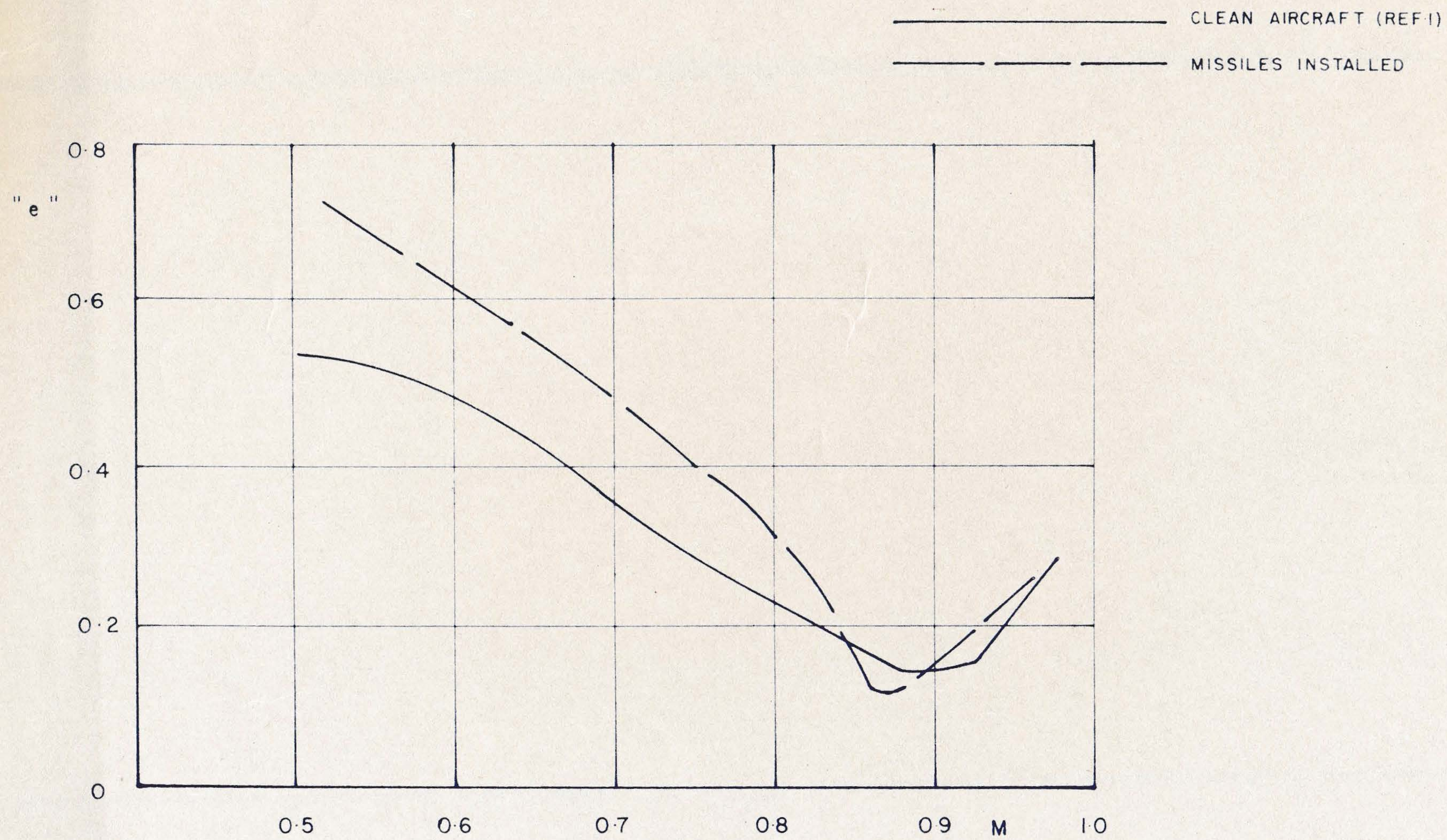

COMPARISON OF INDUCED DRAG EFFICIENCY FACTORS WITH AND WITHOUT MISSILES

NO TAIL CONFIGURATION

FIG· 17

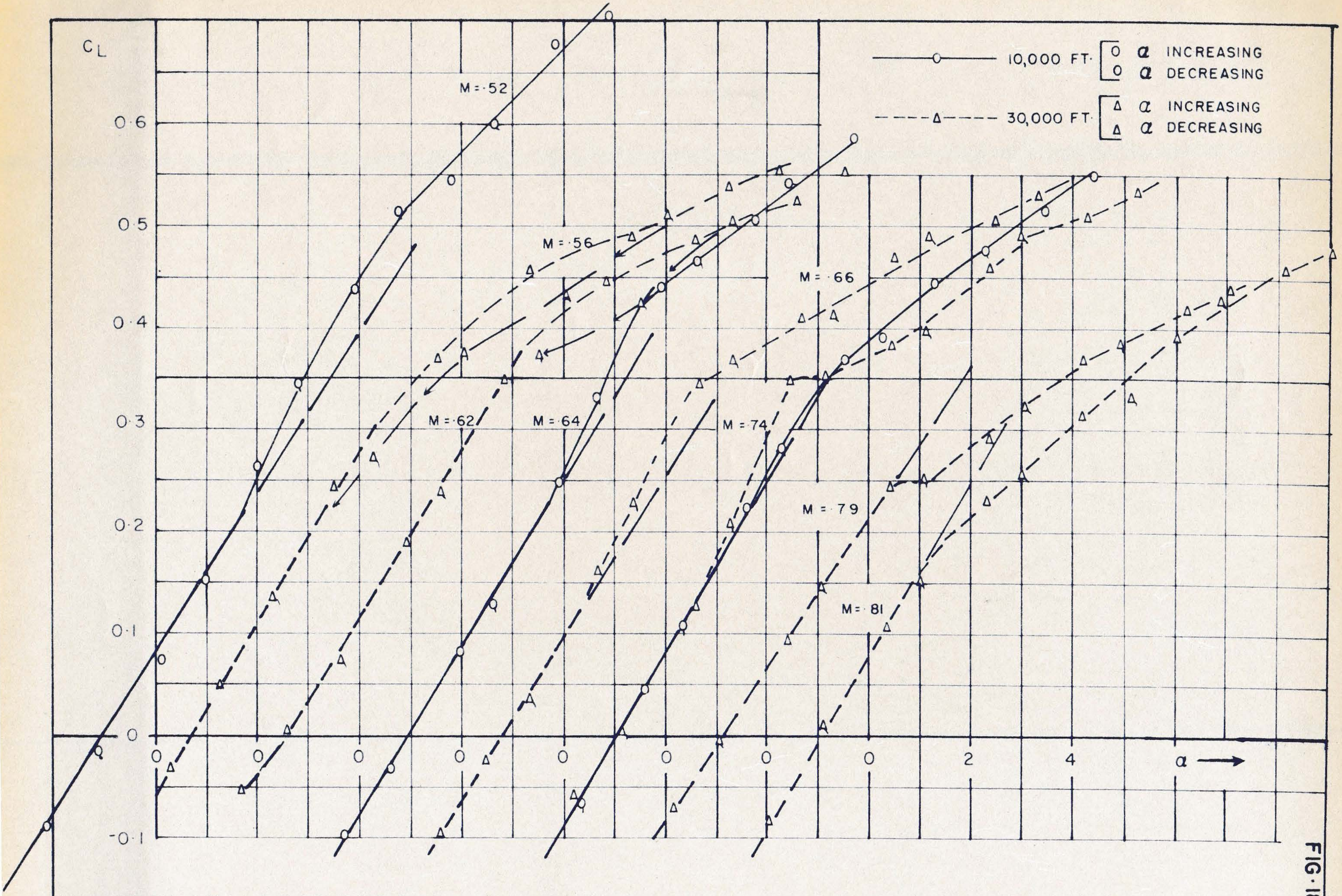

VARIATION OF LIFT COEFFICIENT WITH ANGLE OF ATTACK — COMPLETE AIRCRAFT — MISSILES INSTALLED

FIG·18(a)

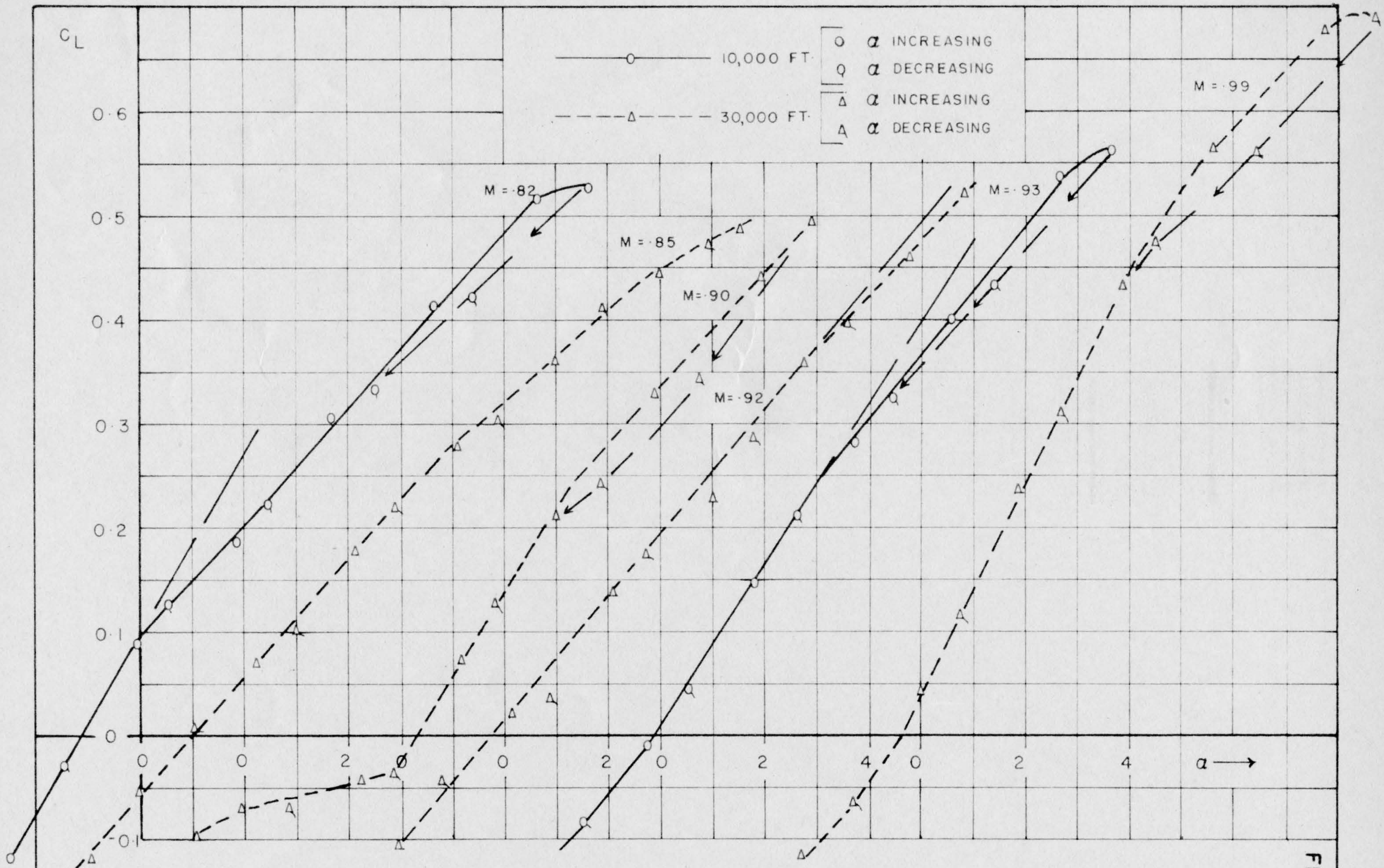

VARIATION OF LIFT COEFFICIENT WITH ANGLE OF ATTACK — COMPLETE AIRCRAFT — MISSILES INSTALLED

FIG. 18(b)

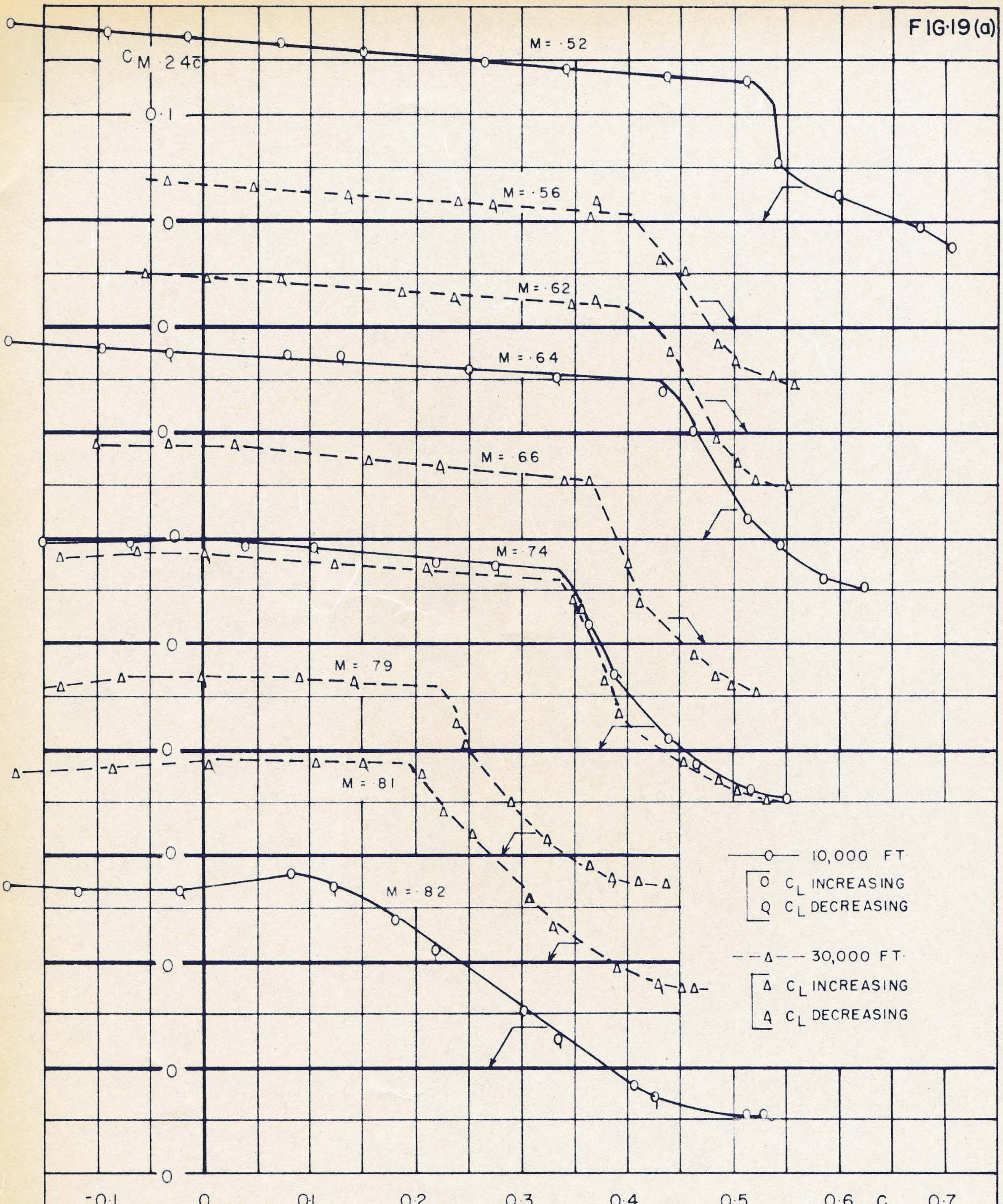

VARIATION OF $C_{M \cdot 24\bar{c}}$ WITH C_L

COMPLETE AIRCRAFT—MISSILES INSTALLED

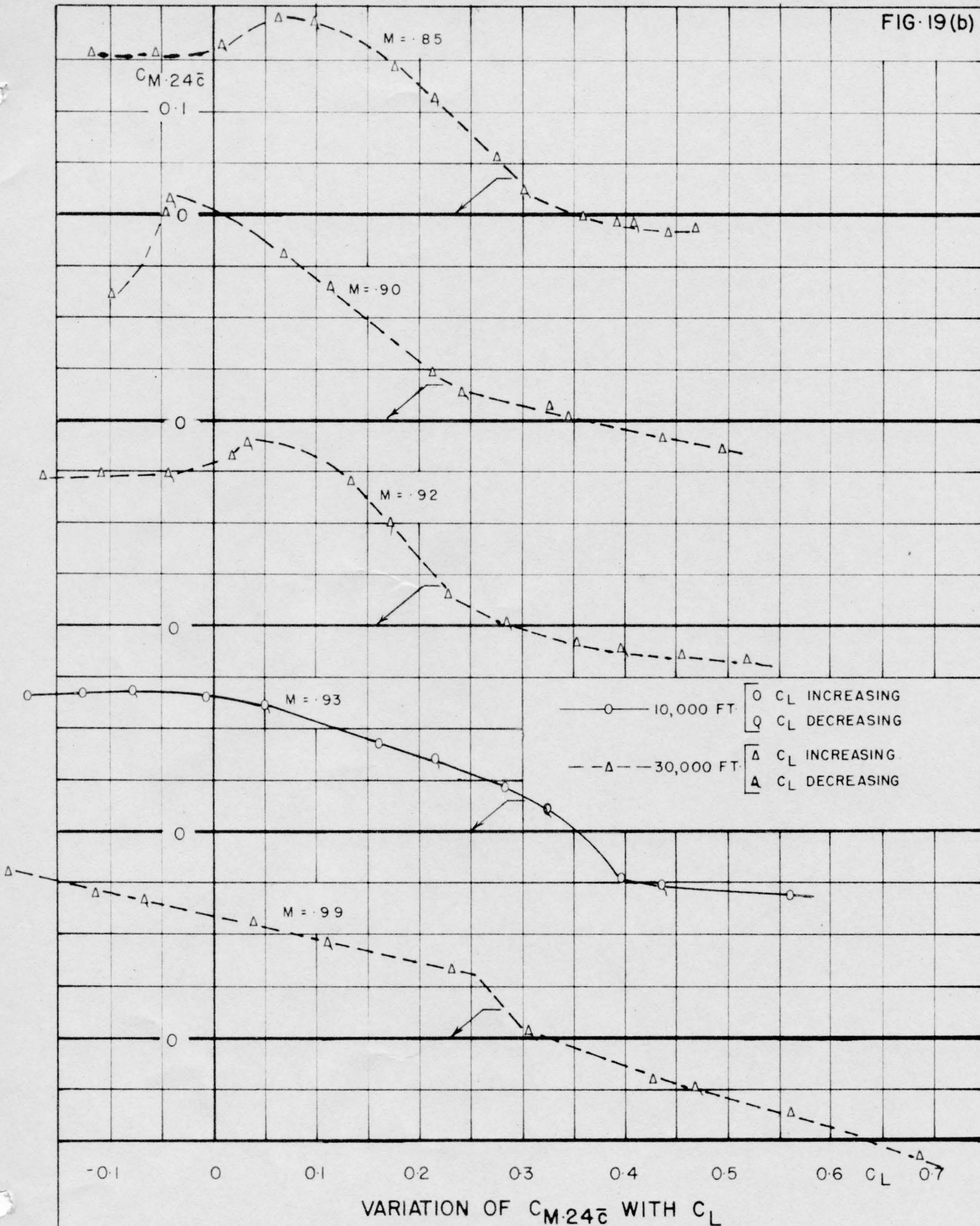

VARIATION OF $C_{M \cdot 24\bar{c}}$ WITH C_L

COMPLETE AIRCRAFT — MISSILES INSTALLED

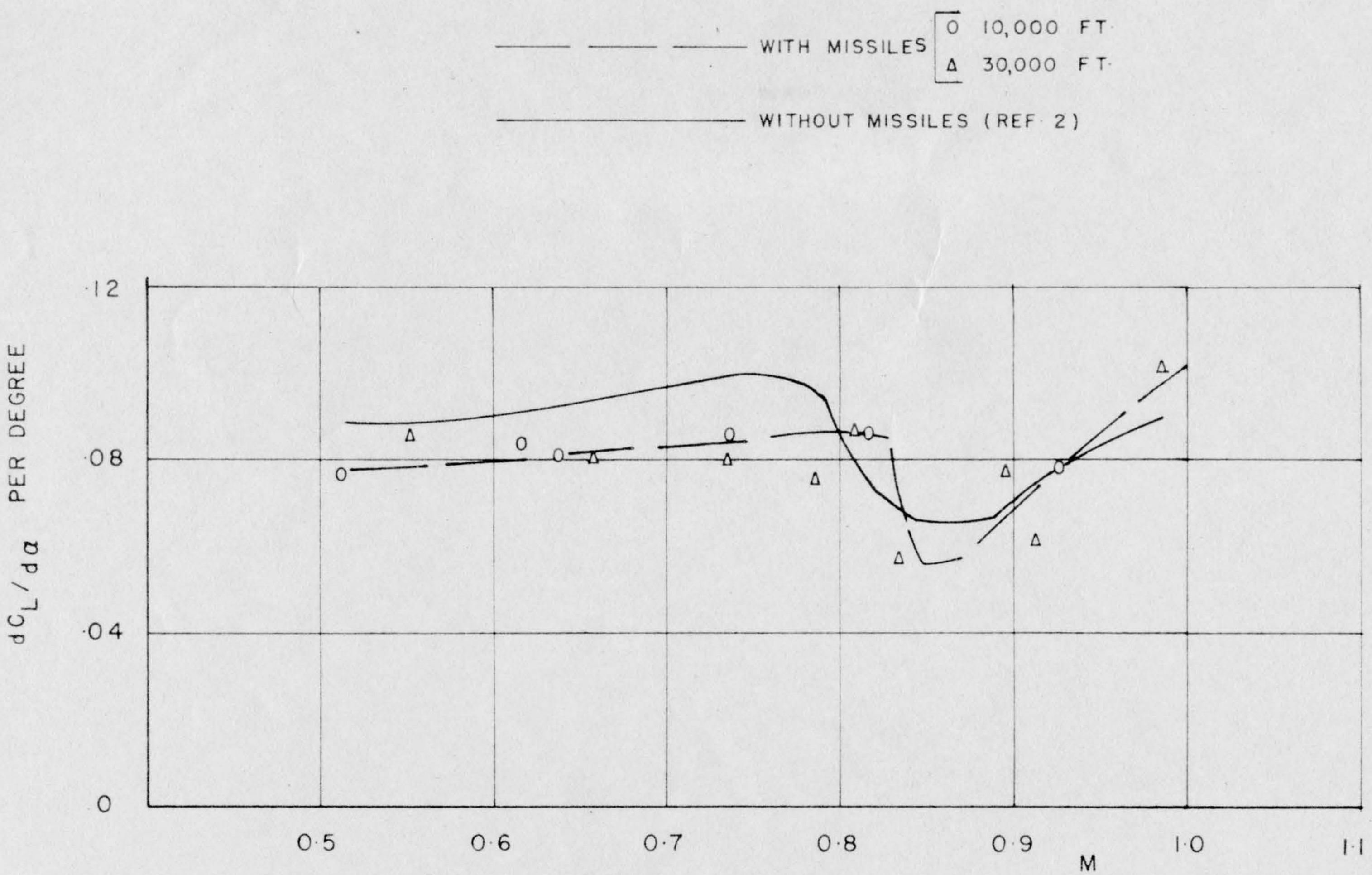

COMPARISON OF LIFT CURVE SLOPES WITH AND WITHOUT MISSILES

COMPLETE AIRCRAFT

FIG. 20

FIG· 21

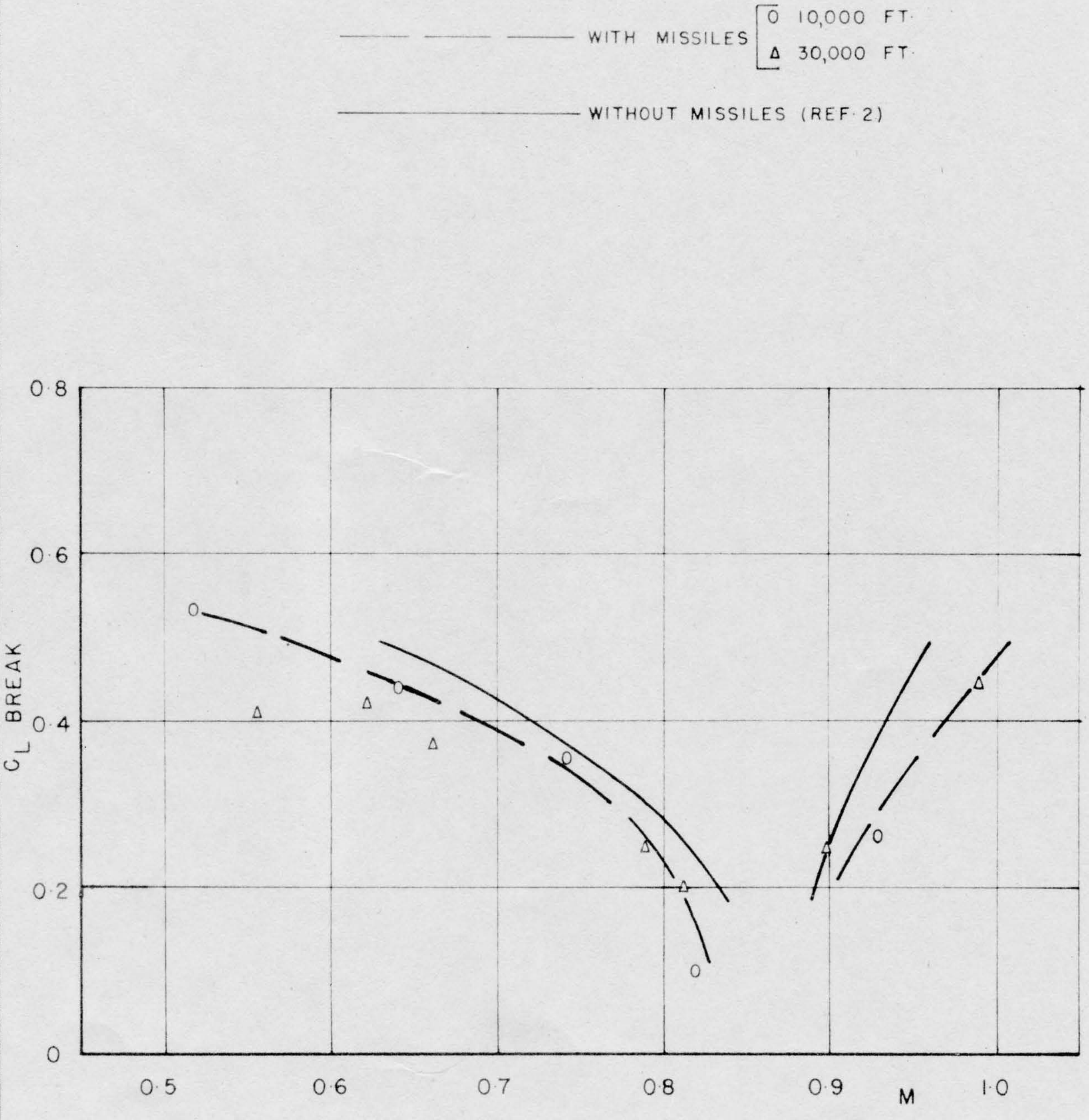

COMPARISON OF LIFT CURVE BREAK WITH AND WITHOUT MISSILES

COMPLETE AIRCRAFT

FIG· 22

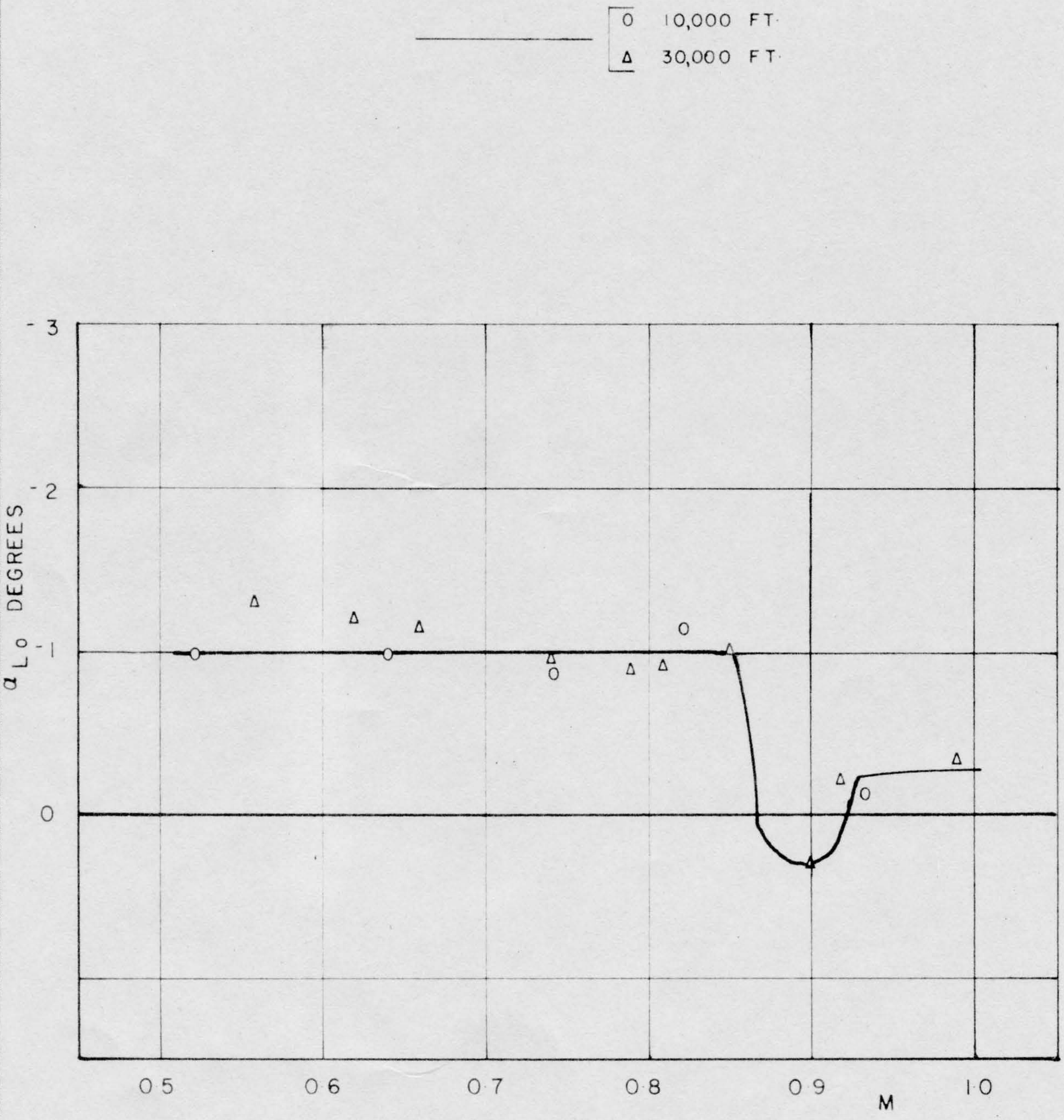

VARIATION OF ANGLE OF ZERO LIFT WITH MACH NUMBER

COMPLETE AIRCRAFT — MISSILES INSTALLED

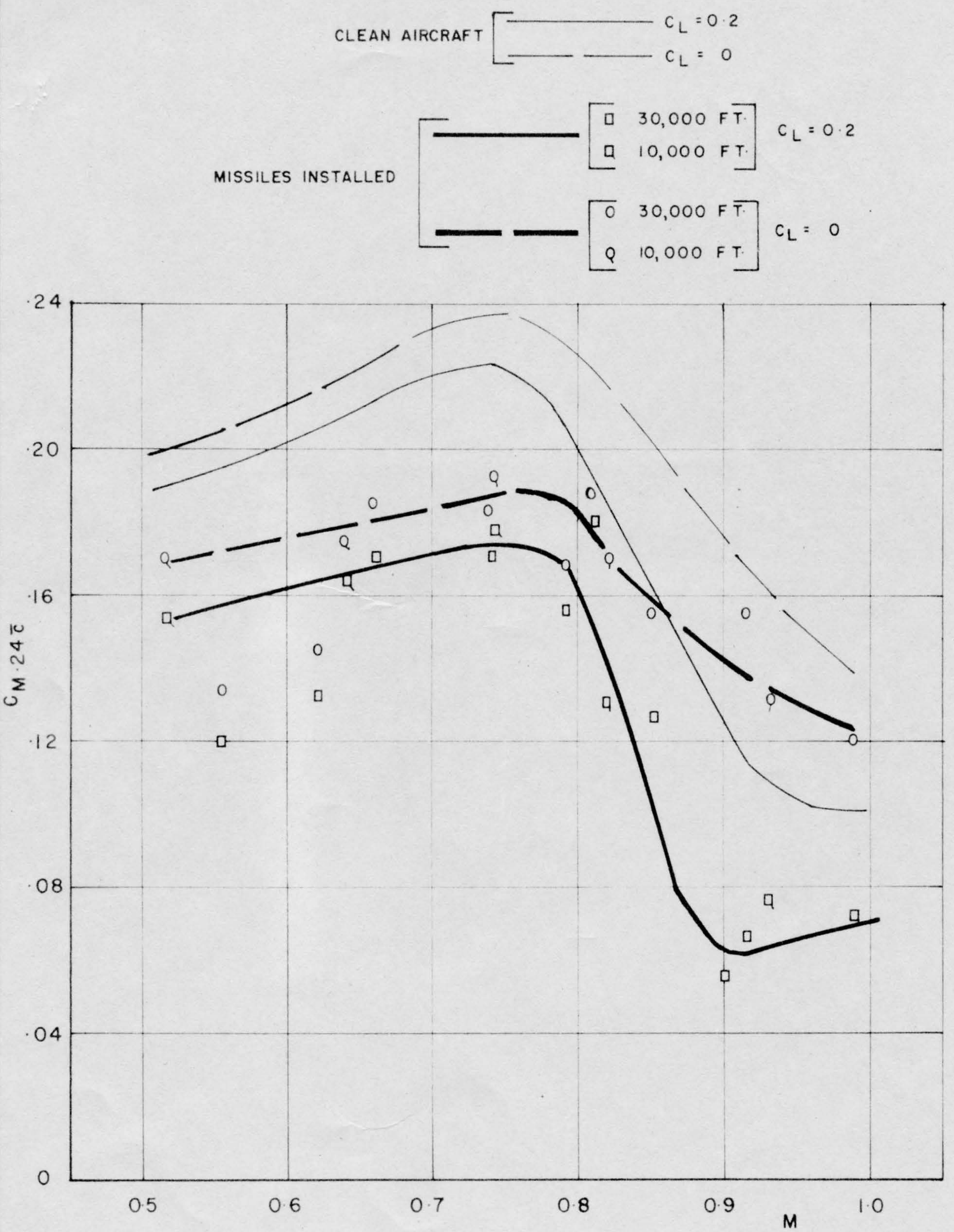

COMPARISON OF $C_{M \cdot 24\bar{c}}$ (CONSTANT C_L) WITH AND WITHOUT MISSILES

COMPLETE AIRCRAFT

N.A.C.A. FR 16 UNCLASSIFIED

Wing Flow Tests to Determine the Effect of the External Stowage of Four N-44 Missiles on the Lift, Drag & Pitching Moment Characteristics of the Avro CF-100.

DATE	ISSUED TO	CLOCK CARD & DEPT. NO.
JUL 1953		
JUL 31 1953		8913A
SEP 4 1953		3721
	D. Nash	8382
OCT 27 1953		
JUN 18 1954		
FEB 14 1958	D. Stewart	